π-Conjugated Poly(pyridine-2,5-diyl), Poly(2,2′-bipyridine-5,5′-diyl), and Their Alkyl Derivatives. Preparation, Linear Structure, Function as a Ligand to Form Their Transition Metal Complexes, Catalytic Reactions, n-Type Electrically Conducting Properties, Optical Properties, and Alignment on Substrates

Takakazu Yamamoto,*,† Tsukasa Maruyama,† Zhen-hua Zhou,† Takayori Ito,† Takashi Fukuda,† Yutaka Yoneda,† Farida Begum,† Tomiki Ikeda,† Shintaro Sasaki,‡ Hideo Takezoe,§ Atsuo Fukuda,§ and Kenji Kubota‖

Contribution from the Research Laboratory of Resources Utilization, Tokyo Institute of Technology, 4259 Nagatsuta, Midori-ku, Yokohama 227, Japan, School of Materials Science, Japan Advanced Institute of Science and Technology, 15 Asahidai, Tatsunokuchi, Ishikawa 923-12, Japan, Department of Organic and Polymeric Materials, Tokyo Institute of Technology, 2-12-1 O-okayama, Meguro-ku, Tokyo 152, Japan, and Faculty of Engineering, Gunma University, Tenjincho, Kiryu 376, Japan

Received November 9, 1993®

Abstract: Dehalogenation polycondensation of corresponding dihalo compounds with a zerovalent nickel complex gives π-conjugated polymers constituted of pyridine units and 2,2′-bipyridine units in high yields. Poly(pyridine-2,5-diyl) (PPy), poly(2,2′-bipyridine-5,5′-diyl) (PBpy), 3-, 4-, and 6-methylated poly(pyridine-2,5-diyl)s (PMePy's), poly(6-hexylpyridine-2,5-diyl) (P6HexPy), poly(3,3′-dimethyl-2,2′-bipyridine-5,5′-diyl) (P3MeBpy), and poly(6,6′-dihexyl-2,2′-bipyridine-5,5′-diyl) (P6HexBpy) are constituted of 42–300 π-conjugated pyridine rings as measured by light-scattering methods. PPy and PBpy have a rigidly linear rodlike structure as revealed by their showing a theoretically limiting ρ_v (degree of depolarization) value of 0.33, and they exhibit a large refractive index increment ($\Delta n/\Delta c = 0.59$ cm^3 g^{-1}) and a large refractive index of $n_D = 2.2$. Stretching of poly(vinyl alcohol) film containing the PPy or PBpy molecules in its surface region affords a polarizer which shows a dichroic ratio of 45. The PBpy molecules stand upright on a carbon substrate in a PBpy film vacuum deposited on the carbon substrate as revealed by electron diffractometry. On the other hand, PBpy molecules in a film vacuum deposited on a glass substrate are oriented in parallel with the surface of the glass substrate as revealed by analysis of optical second-harmonic generation from the PBpy film, which shows alignment of all the PBpy molecules attached to the glass substrate (1 × 1 cm) in a same direction: coordination of a PBpy molecule to the Si–O–H group is proposed to explain such orientation of the PBpy molecules. PPy exhibits fluorescence with a peak at 440 nm in a dilute solution (2 × 10^{-6} M monomer unit), whereas PPy shows an additional excimer-like emission at 550 nm in a saturated solution (0.5 M monomer unit) and PPy and PBpy films emit only the excimer-like emission at 550 nm. Picosecond time-resolved fluorescence also supports the excimer-like fluorescence. PPy, PBpy, and their alkyl derivatives are electrochemically reduced or n-doped more easily than poly(*p*-phenylene) and poly(thiophene-2,5-diyl), reflecting π-electron-deficient nature of the pyridine ring, and E_0 values of −2.2 through −2.5 V *vs* Ag/Ag$^+$ are observed for the polymers; the n-doping and its reverse reaction (n-undoping) are accompanied by a color change (e.g., yellow in the n-undoped state and blue in the n-doped state for PPy and PBpy). Chemically n-doped PPy and PBpy with sodium naphthalide have electrical conductivities of 1.1 × 10^{-1} and 1.6 × 10^{-1} S cm^{-1}, respectively, as measured with compressed powder. On the contrary, PPy, PBpy, and their alkyl derivatives undergo p-doping neither electrochemically nor chemically (e.g., by treatment with AsF_5), reflecting the π-deficient nature of the pyridine ring. PBpy and P6HexBpy form complexes with Ru(II), Ni(II), Ni(0), and Fe(III) species, and cyclic voltammetry of the PBpy–Ru complex reveals electron exchange between the coordinated Ru species, which is considered to occur through the π-conjugation system of the conjugated polymer ligand. The complexes are active for photoevolution of H_2 from aqueous media as well as for reduction of CO_2.

Chemical and physical properties of π-conjugated poly(arylene)s are the subject of recent interest,[1] and a variety of poly(arylene)s including poly(*p*-phenylene) (PPP), poly(thiophene-2,5-diyl) (PTh), and poly(pyrrole-2,5-diyl) have been prepared by various methods.

Among the poly(arylene)s, PPP is constituted of the most fundamental aromatic ring and is considered to have a rigidly linear structure. Actually such a linear structure of PPP has been supported by X-ray diffraction analysis[2] as well as alignment of the PPP molecules perpendicularly to the surface of substrates.[3] However, its very low solubility has prevented its structure, chemical properties, and physical properties as a molecule from being revealed.

On the other hand, poly(pyridine-2,5-diyl) (PPy), constituted of another fundamental aromatic ring, has received much less

† Research Laboratory of Resources Utilization, Tokyo Institute of Technology.
‡ Japan Advanced Institute of Science and Technology.
§ Department of Organic and Polymeric Materials, Tokyo Institute of Technology.
‖ Gunma University.
® Abstract published in *Advance ACS Abstracts*, April 15, 1994.

0002-7863/94/1516-4832$04.50/0

attention[4] when compared with PPP, although it also takes a linear structure similiar to that of PPP and may contribute to understanding the chemical and physical properties of such a linear molecules if it is soluble in solvents.

In our studies on the preparation of poly(arylene)s by dehalogenation polycondensation of dihaloaromatic compounds,[3b,4a,5] which is based on organonickel chemistry[6] and on the chemical and physical properties of poly(arylene)s, we have found that PPy prepared by this method is soluble in some organic and inorganic solvents and PPy as well as its derivatives exhibit interesting chemical and physical properties.

$$n\text{X–Ar–X} + n\text{M} \xrightarrow{\text{catalyst}} \text{(Ar)}_n \qquad (1)$$

M = Mg,[4a,5a] Zn,[5b] or Ni(0)[3b,4b–d,5c]

We now report the preparation of PPy, poly(2,2′-bipyridine-5,5′-diyl) (PBpy), and their derivatives as well as their structure, chemical reactivities, electrical conducting properties, and optical properties. The polymers PBpy and PRBpy (R = Me, *n*-C_6H_{13}) serve as electrically conducting chelating ligands to form complexes with transition metals.

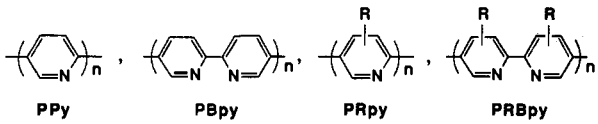

Results and Discussion

Preparation. The dehalogenation polycondensation using zerovalent nickel complexes,

$$n\text{X–Ar–X} + n\text{Ni(0)L}_m \rightarrow \text{(Ar)}_n + {}^n\text{NiX}_2\text{L}_m \qquad (2)$$

Scheme 1

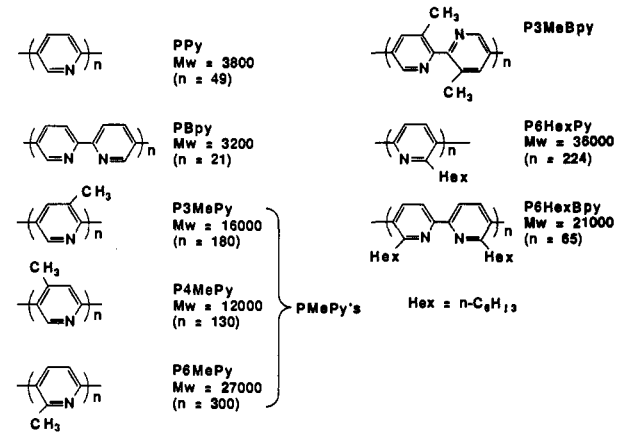

gives the following π-conjugated polymers[7] in high yields as shown in Table 1. The following reaction mechanism involving oxidative addition of Pi ($X(Ar)_iX$) (i = 1, 2, ...) (eq 3), disproportionation (eq 4), and reductive elimination (eq 5) reasonably accounts for the polymerization process.

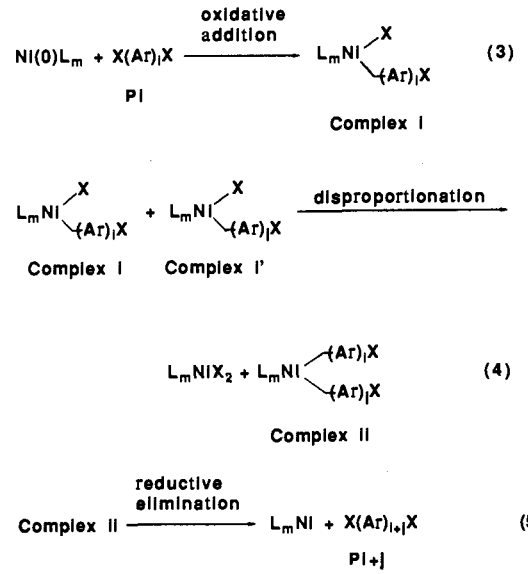

We have proposed, on the basis of kinetics, a similar reaction mechanism for the coupling of ArX to give Ar–Ar by using Ni(0) complexes.[6g] In the mechanism shown above (eqs 3–5), the oxidative addition of aryl halides to the Ni(0) complex[8] and reductive elimination of R–R from diorganonickel NiR_2L_m type complexes[6a–e] are well-known, and disproportionation of organo(halo)nickel(II) complex $NiR(X)L_m$ to NiR_2L_m and NiX_2L_m is also known.[9a] The disproportionation reaction (eq 4) is considered to be facilitated in polar solvents like DMF,[6g] and it corresponds to the suitability of the polar solvents like DMF (Table 1) for the present polymerization.

(1) (a) Skotheim, T. A., Ed. *Handbook of Conducting Polymers*; Marcel Dekker: New York, 1986; Vols. I and II. (b) Salaneck, W. R.; Clark, D. L.; Samuelsen, E. J. E. *Science and Applications of Conducting Polymers*; Adam Hilger: New York, 1990. (c) MacDiarmid, A. G.; Heeger, A. J. *NRL Memo. Rep.* (Proceedings of the Molecular Electron Devices Workshop) **1981**, *AD-A 05816*, 208. (d) Andre, J.-M.; Delhalle, J.; Bredas, J.-L. *Quantum Chemistry Aided Design of Organic Polymers*; World Scientific: London, 1991. (e) Kuzmany, H., Mehring, M., Roth, S., Eds. *Electronic Properties of Conjugated Polymers*; Springer: Berlin, 1987. (f) Bradley, D. D. C.; Mori, Y. In *Electronic Properties of Conjugated Polymers III*; Kuzmany, H., Mehring, M., Roth, S., Eds.; Springer: Berlin, 1989. (g) Collard, D. M.; Fox, M. A. *J. Am. Chem. Soc.* **1991**, *113*, 9414. (h) Guay, J.; Diaz, A.; Wu, R.; Tour, J. M. *J. Am. Chem. Soc.* **1993**, *115*, 1869. (i) Tour, J. M.; Lamba, J. J. S. *J. Am. Chem. Soc.* **1993**, *115*, 4935. (j) Furukawa, Y.; Ohta, H.; Sakamoto, A.; Tasumi, M. *Spectrochim. Acta* **1991**, *47A*, 1367. (k) Seki, K. In *Optical techniques to characterize polymer systems*; Baessler, H., Ed.; Elsevier: Amsterdam, 1989; p 115.

(2) (a) Kovacic, P.; Feldman, M. B.; Kovacic, J. P.; Lando, J. B. *J. Appl. Polym. Sci.* **1968**, *12*, 1735. (b) Froyer, G.; Maurice, F.; Mercier, J. P.; Riviere, D.; Le Cun, M.; Auvray, P. *Polymer* **1981**, *22*, 992. (c) Shacklette, L. W.; Chance, R. R.; Ivory, D. M.; Miller, G. G.; Baughman, R. H. *Synth. Met.* **1980**, *1*, 307. (d) Sasaki, S.; Yamamoto, T.; Kanbara, T.; Morita, A.; Yamamoto, T. *J. Polym. Sci.* **1992**, *30*, 293.

(3) (a) Yamamoto, T.; Kanbara, T.; Mori, C. *Synth. Met.* **1990**, *38*, 399. (b) Yamamoto, T.; Morita, A.; Miyazaki, Y.; Maruyama, T.; Wakayama, H.; Zhou, Z.-H.; Nakamura, Y.; Kanbara, T.; Sasaki, S.; Kubota, K. *Macromolecules* **1992**, *25*, 1214.

(4) (a) Yamamoto, T.; Hayashi, Y.; Yamamoto, A. *Bull. Chem. Soc. Jpn.* **1978**, *51*, 2091. (b) Yamamoto, T.; Ito, T.; Kubota, K. *Chem. Lett.* **1988**, 153. (c) Yamamoto, T.; Maruyama, T.; Kubota, K. *Ibid.* **1989**, 1951. (d) Yamamoto, T.; Ito, T.; Sanechika, K.; Hishinuma, M. *Synth. Met.* **1988**, *25*, 103. (e) Schiavon, G.; Zotti, G.; Bontempelli, G.; Lo Coco, F. *J. Electroanal. Chem. Interfacial Electrochem.* **1988**, *242*, 131. (f) Yamamoto, T.; Ito, T.; Sanechika, K.; Hishinuma, M. *Chem. Ind. (London)* **1988**, 337.

(5) (a) Yamamoto, T.; Yamamoto, A. *Chem. Lett.* **1977**, 353. (b) Yamamoto, T.; Osakada, K.; Wakabayashi, T.; Yamamoto, A. *Makromol. Chem., Rapid Commun.* **1985**, *6*, 671. (c) Yamamoto, T.; Morita, A.; Maruyama, T.; Zhou, Z.-H.; Kanbara, T.; Sanechika, K. *Polym. J.* **1990**, *22*, 187.

(6) (a) Yamamoto, T.; Yamamoto, A.; Ikeda, S. *J. Am. Chem. Soc.* **1971**, *93*, 3350. (b) Yamamoto, T.; Yamamoto, A.; Ikeda, S. *J. Am. Chem. Soc.* **1971**, *93*, 3360. (c) Kohara, T.; Yamamoto, T.; Yamamoto, A. *J. Organomet. Chem.* **1980**, *192*, 265. (d) Komiya, S.; Abe, Y.; Yamamoto, A.; Yamamoto, T. *Organometallics* **1983**, *2*, 1466. (e) Tatsumi, K.; Nakamura, A.; Komiya, S.; Yamamoto, T.; Yamamoto, A. *J. Am. Chem. Soc.* **1984**, *106*, 8181. (f) Zhou, Z.-H.; Yamamoto, T. *J. Organomet. Chem.* **1991**, *414*, 119. (g) Yamamoto, T.; Wakabayashi, S.; Osakada, K. *J. Organomet. Chem.* **1992**, *428*, 223. (h) Semmelhack, M. F.; Ryono, L. S. *J. Am. Chem. Soc.* **1975**, *97*, 3873. (i) Åkermark, B.; Johansen, H.; Roos, B.; Wahlgren, U. *J. Am. Chem. Soc.* **1979**, *101*, 5876.

(7) The dehalogenation polycondensation using Mg also gave PPy;[4a] however, complete transformation of X–Py–X to the intermediate Grignard reagent was somewhat difficult and the polymerization in THF was sometimes accompanied by polymerization of THF.

Table 1. Preparation of PPy and Related Polymers by Dehalogenation Polycondensation of X–Ar–X with a Mixture of $Ni(cod)_2$ and Neutral Ligand L

run	monomer (X–Ar–X)[a]	ligand[b]	reaction conditions: solvent[c]	temp, °C	time, h	yield,[d] %	mol wt[e]	$[\eta]^f$, dL g^{-1}	λ_{max}, nm
1	Br–Py–Br	bpy	DMF	60	2	93	2 700		
2	Br–Py–Br	bpy	DMF	60	4	91	2 400		
3	Br–Py–Br	bpy	DMF	60	8	100	4 300		
4	Br–Py–Br	bpy	DMF	60	16	95	3 800	0.85[g]	373[g]
5	Br–Py–Br	PPh_3	DMF	rt	24	64	1 200		
6	Br–Py–Br	PPh_3	DMF	60	16	95	1 900		
7	Br–Py–Br	PPh_3	HMPA	60	16	95	1 300		374[g]
8	Br–Py–Br	$Ni(PPh_3)_4$[h]	DMF	60	16	59	1 600		
9	Br–Py–Br	$Ni(PPh_3)_4$[i]	DMF	60	16	66	1 400		
10	Br–Py–Br	PPh_3 + mah[j]	DMF	60	16	84			
11	Br–Py–Br	cod	DMF	60	16	97	1 600		
12	Cl–Py–Cl	bpy	DMF	60	16	99	3 300		
13	Cl–Py–Cl	PPh_3	DMF	60	16	87	2 200		
14	Cl–Py–Cl	cod	DMF	60	16	87	2 400		
15	Br–Bpy–Br	bpy	DMF	70	20	95	3 200		373[g]
16	Br–Bpy–Br	PPh_3	DMF	70	28	95	1 200		
17	Br–Bpy–Br	Py	DMF	70	28	92	630		
18	Br–3MePy–Br	bpy	DMF	60	16	80	16 000	1.61[g]	320[g]
19	Br–4MePy–Br	bpy	DMF	60	16	80	12 000	1.01[g]	310[g]
20	Br–6MePy–Br	bpy	DMF	60	16	90	27 000	1.50[g]	340[g]
21	Br–3MeBpy–Br	bpy	DMF	60	16	85			
22	Br–6HexPy–Br	bpy	DMF	60	48	80	36 000		340[g] 321[k]
23	Br–6HexBpy–Br	bpy	DMF	60	48	85	21 000		

[a] X–Py–X = 2,5-dihalopyridine, Br–Bpy–Br = 5,5′-dibromo-2,2′-bipyridine, Br–3MePy–Br = 2,5-dibromo-3-methylpyridine, Br–4MePy–Br = 2,5-dibromo-4-methylpyridine, Br–6RPy–Br = 2,5-dibromo-6-alkylpyridine (R: Me = methyl, Hex = hexyl), Br–3MeBpy–Br = 5,5′-dibromo-3,3′-dimethyl-2,2′-bipyridine, Br–6HexBpy–Br = 5,5′-dibromo-6,6′-dihexyl-2,2′-bipyridine. [b] Bpy = 2,2′-bipyridine, PPh_3 = triphenylphosphine, cod = 1,5-cyclooctadiene, mah = maleic anhydride. 1–1.5 mol of $Ni(cod)_2$/mol of the monomer was added except for run 15, where 2 mol of $Ni(cod)_2$/1 mol of monomer was added. About an equimolar amount of ligand to $Ni(cod)_2$ was added. [c] DMF = *N*,*N*-dimethylformamide, HMPA = hexamethylphosphoric triamide. [d] Yield is calculated on the basis of carbon recovered. [e] Determined by the light scattering method. [f] $[\eta]$ = Inherent viscosity; dL g^{-1} = 100 mL g^{-1}. [g] In HCOOH. [h] $Ni(PPh_3)_4$ prepared *in situ* from $NiCl_2$, Zn, and PPh_3 was used instead of the mixture of $Ni(cod)_2$ and ligand. [i] Isolated $Ni(PPh_3)_4$ was used instead of the mixture of $Ni(cod)_2$ and ligand. [j] Maleic anhydride was added before stopping the polymerization. [k] In C_6H_6.

As the neutral ligand L added to the polymerization system, bpy (runs 1–4 in Table 1) affords PPy's with higher molecular weights than PPh_3 (runs 5–7). The reductive elimination (eq 5) is considered to proceed more easily in *cis*-NiR_2L_2 than *trans*-NiR_2L_2, and obtaining higher molecular weight PPy's in the presence of bpy than in the presence of PPh_3 may be related to taking the cis configuration only in the csae of the bpy chelating ligand; on the other hand, divalent $Ni(X)(Y)(PR_3)_2$ (where X and Y are alkyl, halide, etc, and PR_3 = tertiary phosphine) type complexes usually take trans configurations.[8,9]

Since PPy is not soluble in the polymerization solvents, PPy falls out of the solvent as a precipitate. However, as shown in runs 1–4, an increase in the polymerization time seems to lead to an increase in the molecular weight of PPy, suggesting that the polymerization proceeds even in the propagating species in the precipitate. In the case of PPP prepared by an analogous organometallic process, its molecular weight has not been clarified yet due to the lack of solvent for PPP.

As for the proceeding of the polymerization even in the precipitate, a similar increase of molecular weight after the formation of precipitate has been reported for poly(3-alkylthiophene-2,5-diyl).[3b] PMePy's (runs 18–20) are also insoluble in the polymerization solvent, and obtaining high molecular weight PMePy's indicates such polymerization proceeds more easily in PMePy's having lower crystallinity due to the methyl substituent. Polymerization of the monomer with a longer alkyl chain, a hexyl group, affords similar results (runs 22 and 23). When the polymer has lower crystallinity, the reactants (monomer, Ni(0) complex, etc.) may be able to approach the propagating polymer species through its amorphous or locally solubilized part, thus making the polymerization able to proceed even in the precipitate.

Use of $Ni(PPh_3)_4$ (runs 8 and 9) gives PPy in a lower yield, indicating that blocking of the reaction site of Ni toward X–Ar–X by the four PPh_3 ligands retards the polymerization. The dichloro monomer (runs 12–14) shows polymerization reactivity similar to that of the dibromo monomer. New types of π-conjugated chelating ligand polymers, PBpy, P3MeBpy, and P6HexBpy, are obtained by using 5,5′-dibromo-2,2′-bipyridine and its alkylated compounds as the starting monomers (runs 15, 21, and 23).

Characterization. Data from the elemental analysis agree with the structures of the polymers. The minor content of halogen in the polymers suggests that the dihalogenated propagating species such as P_i or P_{i+j} (eqs 3–5) smoothly undergoes oxidative addition to the $Ni(0)L_m$ complex to give species like complex **I** and/or binuclear nickel complex **III** with a structure $Ni(Ar)_iNi$ bridged by the $(Ar)_i$ group.[10] The main part of the polymer is considered

$$\underset{\text{complex I}}{L_mNi(X)(Ar)_iX} + H^+ \rightarrow H(Ar)_iX \qquad (6)$$

$$\underset{\text{complex III}}{L_m(X)Ni(Ar)_iNi(X)L_m} + H^+ \rightarrow H(Ar)_iH \qquad (7)$$

to be obtained from such chemical species, which will give H-terminated polymers during the workup of the polymers involving treatment of the crude polymer with protic solvents and reagents.

PPy, PBpy, PMePy's, and P3MeBpy are soluble in formic acid and concentrated H_2SO_4. Evaporation of formic acid from the

(8) (a) Hidai, M.; Kashiwagi, T.; Ikeuchi, T.; Uchida, Y. *J. Organomet. Chem.* **1971**, *30*, 279. (b) Fahey, D. R.; Baldwin, B. A. *Inorg. Chim. Acta* **1979**, *36*, 269. (c) Fahey, D. R.; Mahan, J. E. *J. Am. Chem. Soc.* **1977**, *99*, 2501. (d) Parshall, G. W. *J. Am. Chem. Soc.* **1974**, *96*, 2360.

(9) (a) Yamamoto, T.; Kohara, T.; Yamamoto, A. *Bull. Chem. Soc. Jpn.* **1981**, *54*, 1720. (b) *Ibid.* **1981**, *54*, 2010. (c) *Ibid.* **1981**, *54*, 2161.

(10) A 1:2 molar reaction between 4,4′-dibromobiphenyl and a zerovalent nickel complex (a mixture of $Ni(cod)_2$ and $2PEt_3$) actually led to the formation of a complex of type complex III, $(PEt_3)_2Ni(Br)–C_6H_4–C_6H_4–Ni(Br)(PEt_3)$, which was isolated and characterized by elemental analysis and X-ray crystalography (Kim, Y.-J.; Sato, R.; Maruyama, T.; Osakada, K.; Yamamoto, T. *J. Chem. Soc., Dalton Trans.*, in press).

formic acid solutions of these polymers gives the original polymer, as proved by IR spectrometry, and thus indicates that formic acid essentially works as a solvent. On the other hand, these polymers seem to be dissolved in concentrated H_2SO_4 as salts with H_2SO_4. P6HexPy and P6HexBpy are soluble in most organic solvents including $CHCl_3$, THF, benzene, formic acid, and hexamethylphosphoric triamide (solubility = 200–300 mg cm^{-3} for these solvents). Enhancement of solubilities of poly(arylene)s by introducing an alkyl substituent and without loosing the essential π-conjugation along the polymer chain has been reported.[11] Determination of the molecular weight of P6HexPy by light scattering by using two kinds of solvents, formic acid and chloroform, gives essentially the same value (37 000 (DP = 230) in formic acid and 36 000 (DP = 220) in chloroform, respectively). The light scattering method also reveals that P6HexPy has a monodispersed relatively narrow molecular weight distribution with a M_z/M_w value of about 2 (M_Z = Z-average molecular weight; M_w = weight-average molecular weight).

In cases of PPy, PMePy's, and P6HexPy, they contain both the head-to-tail H–T and head-to-head H–H units. As for

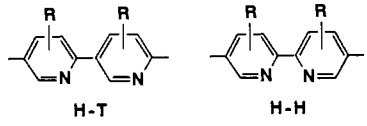

P3MePy and P6HexPy, the H–T to H–H ratios are determined by comparing their ^{1}H-NMR spectra with those of P3MeBpy (Figure 1)[12a] and P6HexBpy, and the ratios[13] thus obtained are

$$\text{for P3MePy H–T/H–H} = 65/35 \quad (8)$$

$$\text{for P6HexPy H–T/H–H} = 55/45 \quad (9)$$

In the case of PPy, it was difficult to determine the H–T/H–H ratio from ^{1}H-NMR; however, the above data (eqs 8 and 9) suggest that PPy is also constituted of H–T and H–H units. The considerably lower coordinating ability of PPy to form metal complexes than PBpy (*vide infra*) suggests a relatively low content of the H–H unit. A mixed coupling reaction between 2-bromopyridine and 3-bromopyridine by using an Ni(0) complex affords the following mixture

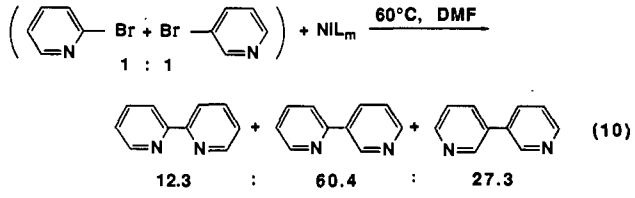

and the preferential formation of 2,3′-bipyridine is consistent

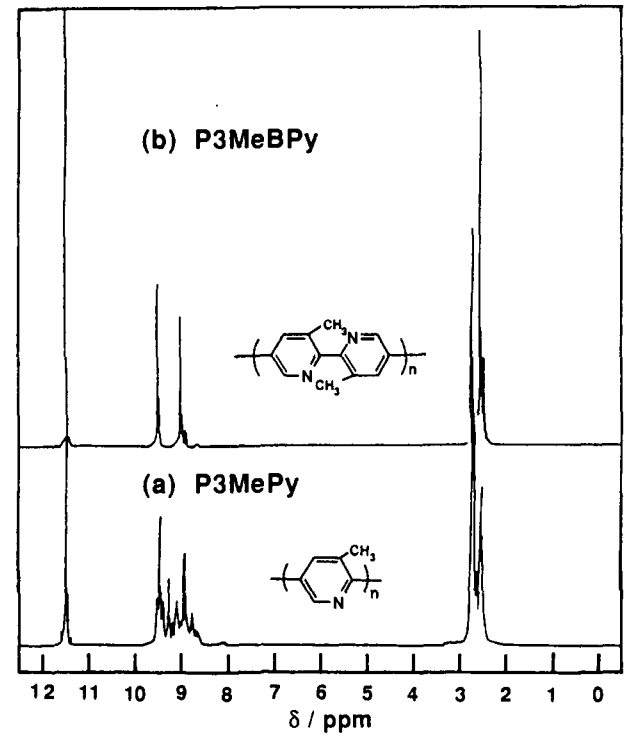

Figure 1. ^{1}H-NMR spectra of (a) P3MePy and (b) P3MeBpy in CF_3-COOD at room temperature.

with the assumption that PPy mainly consists of the H–T unit. In eq 10, 3,3′-bipyridine is formed in a higher ratio than 2,2′-bipyridine, which is consistent with the previously reported higher reactivity of the C–Br bond at the 3-position than that at the 2-position.[14]

IR spectra of the polymers are reasonable for their structures. IR spectra of PBpy, P3MeBpy, and P6HexBpy resemble those of PPy, P3MePy, and P6HexPy respectively, although some differences are observed in the regions of δ(C–H) out-of-plane vibration, δ(CH_3) vibration, and δ(CH_2) vibration between the polypyridine type polymers and polybipyridine type polymers. Detailed NMR and IR data for the polymers are given in the supplementary material.

All the polymers have high thermal stability. TGA indicates that no thermal degradation of PPy and PBpy takes place below 270 °C and their residual weight at 900 °C is about 75%. Even P6HexPy having the alkyl substituent has high thermal stability, showing a residual weight of 95 and 47% at 450 and 900 °C, respectively.

PPy and PBpy give rise to a relatively sharp (half-width = 49 nm or 3500 cm^{-1} (0.44 eV)) single π–π* absorption peak at 373 ± 1 nm or 3.32 ± 0.01 eV in formic acid,[4b,12b] and the peak position is essentially unvaried with the change of the molecular weight (M_w) of PPy in a range of M_w = 1200–3800. The π–π* transition energy of PPy is comparable to that of PPP (λ_{max} = ca. 380 nm or 3.26 eV measured in the solid state) prepared by the organometallic process.[4a] Band gaps of PPy and PBpy estimated from the edge (430 nm) of the absorption spectrum are 2.88 eV.

Introduction of the alkyl substituent causes a shift of the π–π* absorption to shorter wavelength by 30–60 nm (Table 1). A similar hypsochromic effect of the substituent (presumably by disturbing the coplanarity of the π-conjugated polymers) has been reported for poly(thiophene-2,5-diyl).[3b,15] Among PMePy's, P6MePy exhibits the lowest hypsochromic effect probably due

(11) (a) Yamamoto, T.; Sanechika, K. *Chem. Ind. (London)* **1982**, 301. (b) Yamamoto, T.; Sanechika, K.; Yamamoto, A. US Pat. 4521589, 1985. (c) Elsenbaumer, R. S.; Jen, K. Y. J.; Oboodi, R. *Synth. Met.* **1986**, *15*, 169. (d) Rühe, J.; Ezquerra, T.; Wegner, G. *Makromol. Chem., Rapid Commun.* **1989**, *10*, 103. (e) Kaeriyama, K.; Sato, M. *Makromol. Chem., Rapid Commun.* **1989**, *10*, 171.

(12) (a) Maruyama, T.; Zhou, Z.-H.; Kubota, K.; Yamamoto, T. *Chem. Lett.* **1992**, 643. (b) Yamamoto, T.; Maruyama, T.; Ikeda, T.; Sisido, M. *J. Chem. Soc., Chem. Commun.* **1990**, 1306. (c) Yamamoto, T.; Zhou, Z.-H.; Kanbara, T.; Maruyama, T. *Chem. Lett.* **1990**, 223. (d) Yamamoto, T.; Yoneda, Y.; Maruyama, T. *J. Chem. Soc., Chem. Commun.* **1992**, 1652.

(13) More detailed analysis of the ^{1}H-NMR data based on triad and tetrad units may become possible by analyzing the complex peak pattern of the pyridine protons (e.g., Figure 1); such analysis has been carried out for poly(3-alkylthiophene-2,5-diyl): (a) Souto, Maior, R. M.; Hinkelmann, K.; Eckert, H.; Wudl, F. *Macromolecules* **1990**, *23*, 1268. (b) McCullough, R. D.; Lowe, R. D. *J. Chem. Soc., Chem. Commun.* **1992**, 70. (c) Mao, H.; Xu, Bai.; Holdcroft, S. *Macromolecules* **1993**, *26*, 1163.

(14) (a) Tiecco, M.; Testaferri, L.; Tingoni, M.; Chianelli, D.; Montanucci, M. *Synthesis* **1984**, 736. (b) Parham, W. E.; Piccilli, R. M. *J. Org. Chem.* **1977**, *42*, 257.

(15) Yoshino, K.; Onoda, M.; Love, P.; Sugimoto, R. *Jpn. J. Appl. Phys.* **1987**, *26*, L2046. (b) Hotta, S. *Synth. Met.* **1987**, *22*, 103.

Scheme 2

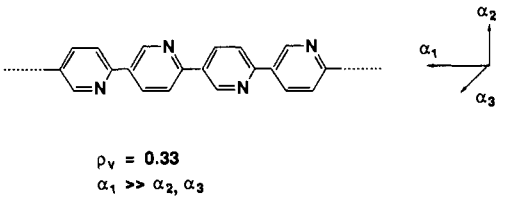

to less steric repulsion between the Me groups in P6MePy than in P3MePy and P4MePy. A CPK molecular model of form b of P6MePy indicates minor steric repulsion between the monomer units.

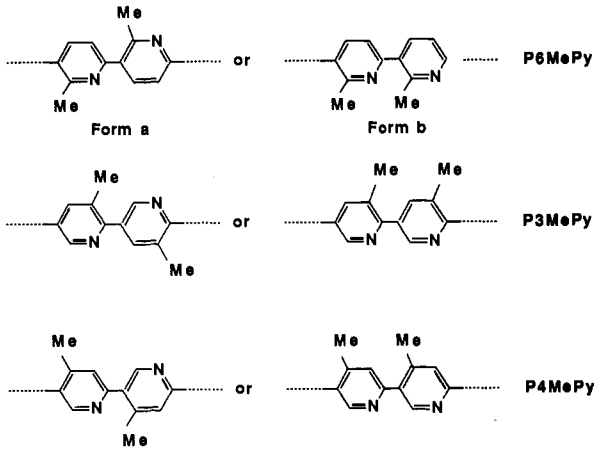

Linear Structure and Alignment of Molecules. Irradiation with a polarized Ar^+ laser (488 nm) of the formic acid solution of PPy and PBpy reveals that the polymers give a very large degree of depolarization of the polarized laser with a ρ_v value[16] of 0.33, which agrees with the theoretical limiting value of $\rho_v = {}^1/_3$ calculated for a molecule in which the polarizability along a rod axis direction (α_1) is very large whereas the polarizability along the other two directions (α_2 and α_3) is negligible compared with α_1.[16] The observed ρ_v value is, to our knowledge, the largest value reported, and the results strongly suggest that PPy and PBpy take a rodlike rigid linear structure having a π-conjugation system with mobile electrons along the polymer chain (presumably the direction of α_1). Due to the presence of mobile electrons along the polymer chain, PPy exhibits a very large refractive index increment of $\Delta n/\Delta c = 0.59$ cm^3 g^{-1} in formic acid, which has n_D of 1.37. The $\Delta n/\Delta c$ value is much larger than those of usual non-π-conjugated polymers ($\Delta n/\Delta c = 0.1$–0.2 cm^3 g^{-1}) and fairly large compared to that of poly(3-hexylthiophene-2,5-diyl) ($\Delta n/\Delta c = 0.35$ cm^3 g^{-1}),[3b] having alkyl substituents. Film of PPy exhibits a very large refractive index of $n_D = 2.2$, a value somewhat lower than that of diamond $n_D = 2.4$.

In contrast to PPy and PBpy, PMePy's, P6HexPy, and P6HexBpy with large molecular weights give ρ_v values of almost 0, indicating that these molecules take essentially a random-coil like structure as a whole molecule probably due to steric repulsion between the alkyl substituents, twisting out of the π-conjugated plane, and/or bowing of the long molecular chain.[16c] That P3MePy takes a locally linear structure has been confirmed by using the low molecular weight (M_w = 770, n = ca. 9) part of P3MePy extracted by hot $CHCl_3$, which shows the ρ_v value of 0.27 in formic acid. P3MePy film has an n_D value of 1.70. A copolymer constituted of pyridine-2,5-diyl units and pyridine-2,6-diyl units prepared by the reaction shown in eq 11 and having

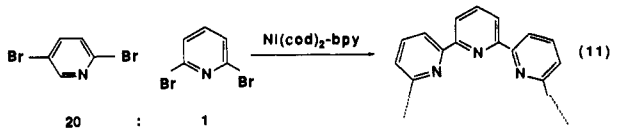

a relatively low molecular weight (M_w = 950, number of pyridine unit = ca. 12) exhibits the π–π^* absorption peak at shorter wavelength (λ_{max} = 353 nm in formic acid) and gives a lower $\Delta n/\Delta c$ value of 0.34 cm^3 g^{-1} and a smaller ρ_v value of 0.15 than compared with PPy. Breaking the π-conjugation and bending the molecule at the pyridine-2,6-diyl unit account for the results. A similar effect of the incorporation of nonconjugated units into the π-conjugated polymer to cause a similar hypsochromic shift of the π–π^* absorption band has been reported for copolymers of π-conjugated thiophene-2,5-diyl and non-π-conjugated thiophene-2,4-diyl units.[17]

Because of the linear structure of PPy and PBpy, they are aligned in stretched film as well as on substrates. As shown in Figure 2a, painting of poly(vinyl alcohol) (PVA) film with a formic acid solution of PPy and drying the film gives the PVA film containing the linear PPy molecules in the surface region. Stretching the film is expected to lead to the alignment of the PPy molecules as shown in Figure 2b, and actually, irradiation of the film with polarized light (Figure 2c) reveals a strong dichroism (or dependence of the absorbance on the angle θ in Figure 2c) as shown in Figures 3 and 4. In Figures 2 and 4, the stretching ratio R_s and the dichroic ratio R_d are defined as

$$R_s = R_\parallel/R_\perp \quad \text{(Figure 2a,b)} \tag{12}$$

$$R_d = A_\parallel/A_\perp = \underset{A = \text{absorbance}}{A_0/A_{90}} \quad \text{(Figures 2c and 3)} \tag{13}$$

The results depicted in Figures 3 and 4, which show such an unusually large dichroic ratio R_d of 40–45, support the alignment of the PPy molecules on the stretched PVA film and reveal that larger dichroic ratios are obtained with PPy's having larger molecular weights. PBpy (with 42 pyridine rings (Scheme 1)) gives, in the PVA film, an R_d value almost the same as that observed with PPy with n value of 49 (Figure 4). Because of the strong dichroism, the stretched film serves as a polarizing film; for example, two overlapped PVA–PPy films with a 90° angle between the stretching directions of the two films cut light at about 400 nm almost completely whereas light at 400 nm passes through two similarly overlapped films with a 0° angle between the stretching directions of the two films. The R_d value for the PVA–PPy film is stable and unvaried even after leaving the film at room temperature for 4 years.

Casting a homogeneous formic acid solution containing PVA and PPy gives a free-standing film containing PPy molecules in bulk PVA, and stretching of the film also affords a film showing dichroism. However, the R_d value of this stretched film is considerably lower (R_d = 2.5, 3.2, and 4.4 at R_s = 2.0, 5.0, and 10.2, respectively), and the difference in the R_d values between the two types of stretched films may be attributed to an excellent special anchoring effect of the surface of the PVA film for alignment of the linear PPy molecules and/or a difference in the nature of the disorder and ordering between the PPy molecules in the surface region (2D disorder and ordering, Figure 2a,b) and those in the bulk (3D disorder and ordering).

Figure 5 (top) shows the electron difraction (ED) pattern of a PBpy film (thickness = 60 nm) formed on a carbon substrate

(16) (a) Kubota, K.; Urabe, H.; Tominaga, Y.; Fujime, S. *Macromolecules* **1984**, *17*, 2096. (b) Kubota, K.; Chu, B. *Biopolymers* **1983**, *22*, 1461. (c) Zero, K.; Aharoni, S. M. *Macromolecules* **1987**, *20*, 1957. (d) Saito, N. *Kobunshi Butsurigaku* (*Polymer Physics*); Shokabo: Tokyo, 1976; pp 181, 210. $\rho_v = 3\delta^2/(5 + 4\delta^2)$, where $\delta^2 = \{(\alpha_1 - \alpha_2)^2 + (\alpha_2 - \alpha_3)^2 + (\alpha_3 - \alpha_1)^2\}/2(\alpha_1 + \alpha_2 + \alpha_3)^2$; under the conditions of $\alpha_1 \gg \alpha_2$ and α_3, δ^2 and ρ_v become 1 and ${}^1/_3$, respectively. Poly(1,4-phenyleneterephthalimine) or Kevlar having a rather rigid linear structure exhibits ρ_v values of 0.175 and 0.11 at M_w values of 4500 and 35 000, respectively.[16c]

(17) (a) Yamamoto, T.; Sanechika, K.; Yamamoto, A. *Bull. Chem. Soc. Jpn.* **1983**, *56*, 1497. (b) Sanechika, K.; Yamamoto, T.; Yamamoto, A. *J. Polym. Sci., Polym. Lett. Ed.* **1982**, *20*, 365.

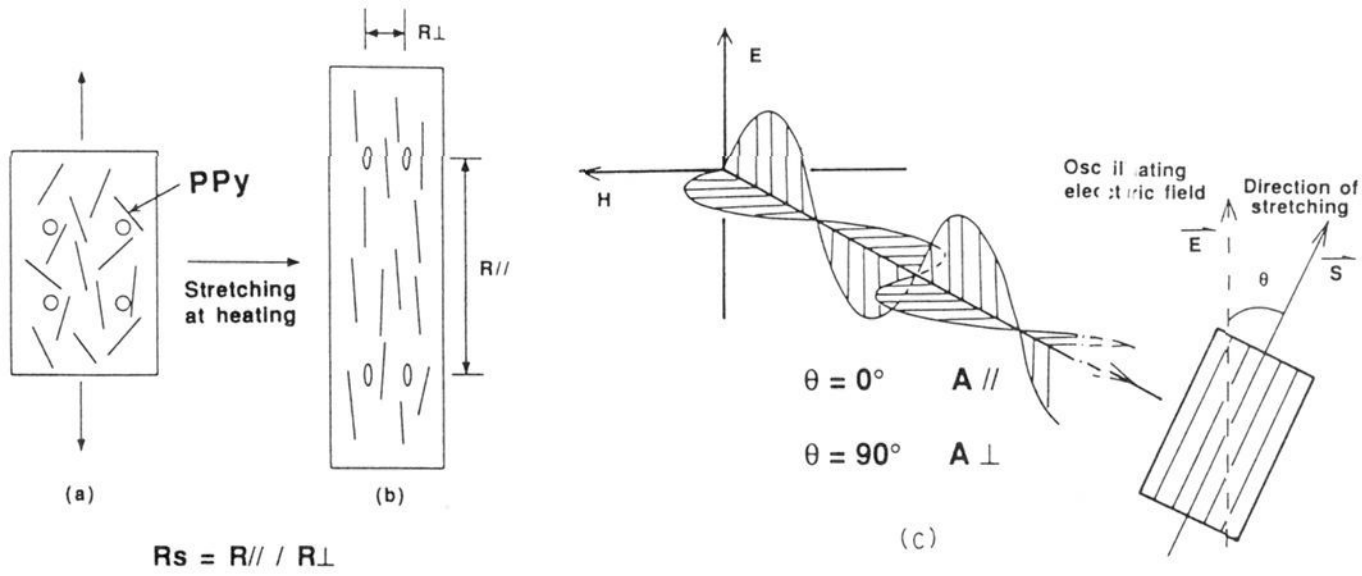

Figure 2. Stretching of PVA film containing linear PPy molecules in its surface region, definition of R_s (Figure 2a,b), and irradiatic ın of polarized light on the stretched film (Figure 2c). The four O marks are made at the corners of a square (Figure 2a.) to determine the R_s value (F igure 2b). The film was obtained by painting the PVA film with a formic acid solution of PPy, drying the film under v acuum, and stretching the P VA film.

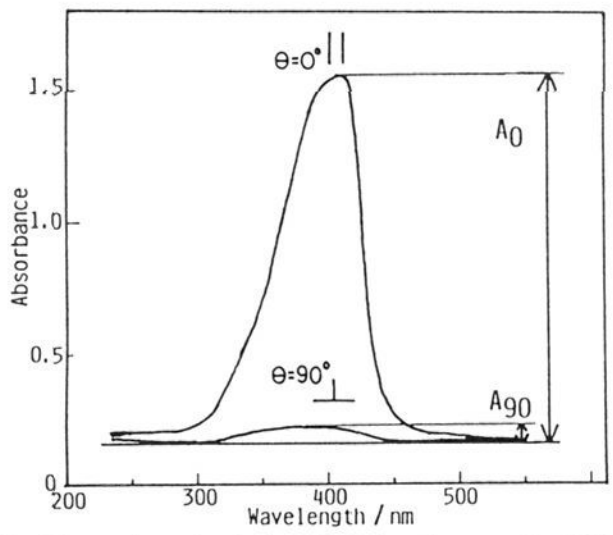

Figure 3. Absorption of polarized light by the stretched PVA–PPy film.

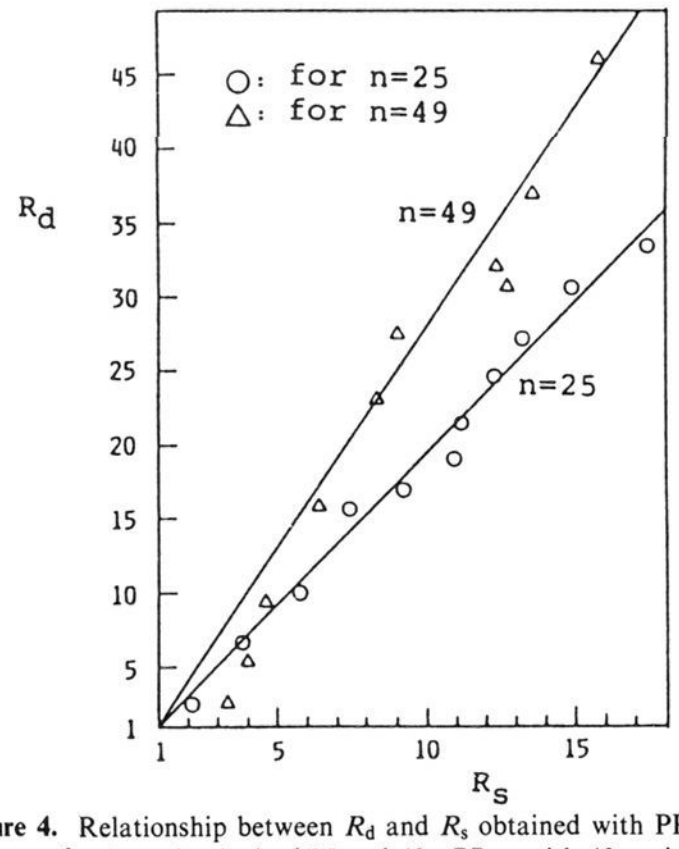

Figure 4. Relationship between R_d and R_s obtained with PPy with n (degree of polymerization) of 25 and 49. PBpy with 42 pyridine rings gives almost the same results obtained with PPy with the n value of 49.

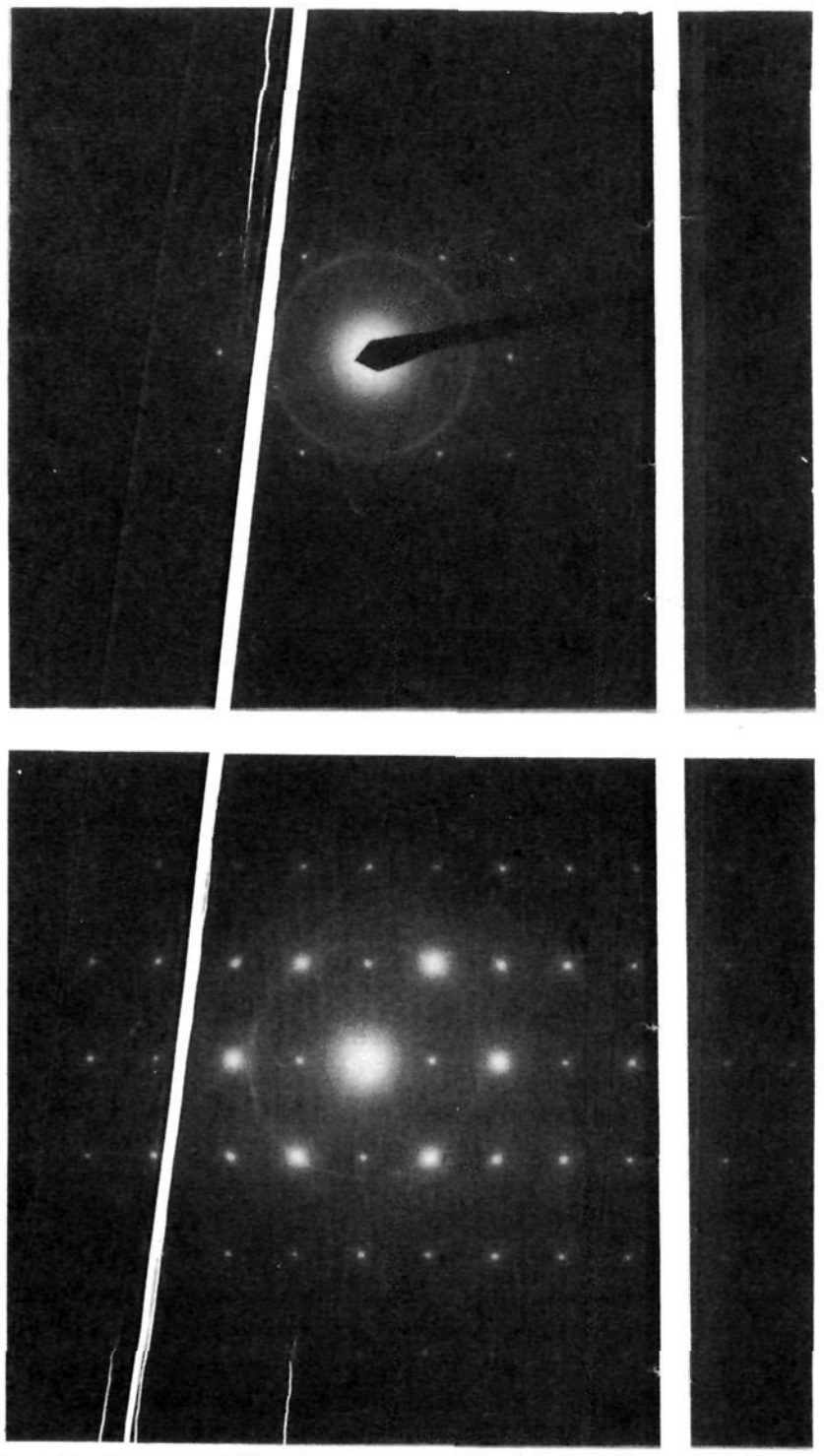

Figure 5. El ectron diffraction pattern of (top) PBpy film and (bottom) PPP film (f rom ref 3) vacuum deposited on a carbon sut ıstrate.

by vacuum deposition. The ED pattern of the vacuum-deposited thin film of PPP[3] is also shown in Figure 5 for comparison. The ED patterns shown in Figure 5 are taken by using an electron beam (60 keV corresponding to a wavelength of 0.0050 nm) irradiated perpendicularly to the carbon substrate. The ED pattern of the PPP film has been reasonably accounted for by assuming that the PPP molecules stand upright as depicted in Figure 6b to form an orthorhombic packing;[3] the orthorhombic packing of PPP has been extensively studied by po wder X-ray diffractometry.[2]

The observation of analogous regular spots in the ED pattern of the vacuum-deposited PBpy suggests that the PBp y molecules also stand upright on the carbon substrate (Figure 6a) to form an orthorhombic packing, although the observation of a smaller number of the regular diffraction spots than that ob served with

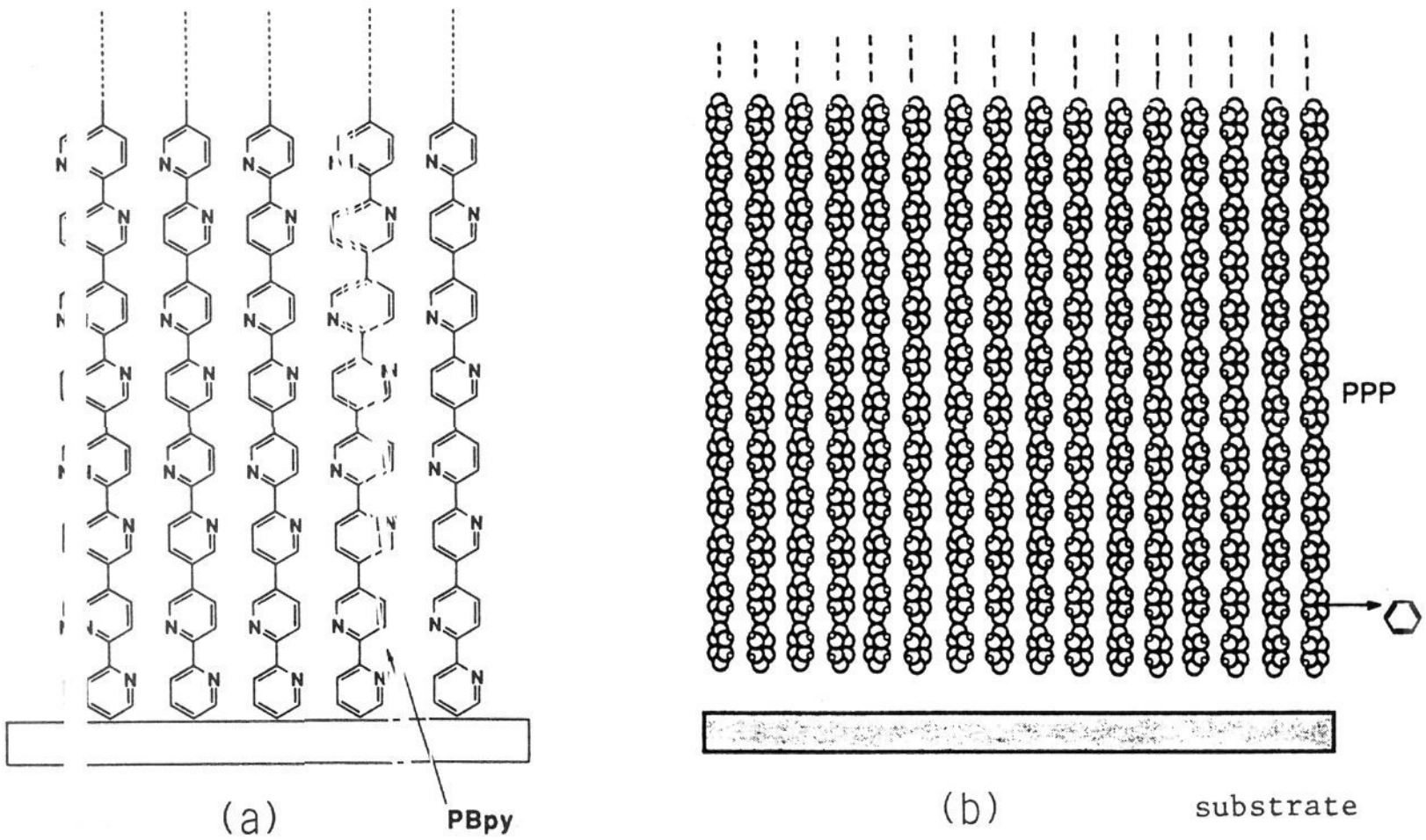

Figure 6. Perpendicular orientation of (a) PBpy and (b) PPP. The detailed packing structure in the *ab* plane and twisting of the aromatic rings are neglected for simplification.

the PPP film indicates a lower degree of crystallinity[18] of the PBpy film presumably due to a less regular and less linear structure of PBpy than that of PPP. For example, PBpy may have irregularities due to the presence of s-cis and s-trans stereoisomeric bonding and nonlinearity due to the presence of N in the six-membered aromatic ring. As a polymerized powder, the sample of PBpy seems to have a monoclinic crystal structure, whose detailed analysis will be reported elsewhere.

As for PPP, it is reported that PPP's with molecular weights of 1500–2000, corresponding to a degree of polymerization of about 20 and a chain length of 8–10 nm, can be vaporized under vacuum.[19] If PBpy has volatileness similar to that of PPP, the PBpy molecules in the vacuum-deposited thin film are also considered to have about 20 pyridine rings and a length of 8–10 nm. Therefore, the thickness (60 nm) of the PBpy film is considered to correspond to an accumulation, on the average, of about 6–8 layers of the PBpy molecules, and observation of the regular clear spots suggests that not only the first PBpy layer directly contacted with the surface of the substrate but also the PBpy molecules in the upper layers are oriented perpendicularly to the surface of the substrate.

The lateral dimensions of the orthorhombic unit cell of the vacuum-deposited PBpy (the *c* axis is the direction of the polymer chain) are 0.81 nm (*a*) and 0.57 nm (*b*), respectively. The values are somewhat larger than the *ab* parameters of PPP and PTh (*a* = 0.78 nm, *b* = 0.56 nm).[2,3,20] The spots shown in Figure 5a disappeared after long irradiation by the electron beam, indicating degradation of the oriented structure by the long irradiation with the electron beam. Use of PPy, instead of PBpy, in the vacuum deposition also gives a similar film; however, its ED pattern exhibits only much less sharp dim spots due to the less regular structure of PPy. The vacuum deposition of PPP to a gold substrate also leads to a similar orientation of the PPP molecules perpendicular to the surface of the substrate.[3] However, in the case of PBpy, the film vacuum-deposited on the gold substrate does not give rise to a clear ED spot. Interaction of the PBpy molecule with the gold substrate through partial coordination of PBpy to gold may be the reason for the difficulty in making the oriented structure.

Vacuum deposition of PBpy on a glass substrate causes another type of alignment of the PBpy molecules on the surface of the substrate as found by using the SHG (optical second-harmonic generation) technique.[21]

Although PPP and PPy films vacuum deposited on the glass substrate are SHG inactive, similarly vacuum-deposited PBpy film is SHG active, indicating that the PBpy molecules take a special alignment on the glass substrate to afford a domain which has asymmetry in inversion. The intensity of the SH light (I_{SH}) from the glass vacuum-deposited PBpy film is much stronger than the background SH light from the glass substrate and proportional to the second power of the intensity of the irradiated laser (I_e), $I_{SH} \propto I_e^2$. A detailed study of SHG has been carried out by irradiation with a laser (1064 nm) and detection of the SH light in P–P (irradiation light = P polarized light; detected SH light = P component of the SH light), S–S, S–P, and P–S combinations as shown in Figure 7, and the obtained results are shown in Figure 8. The SH intensity is predominantly observed in the P–P combination, and the SH intensities in the other three combinations are smaller by 1 order of magnitude, implying that there exists a main nonlinear susceptibility component perpendicular to the surface plane.

As is clear from Figure 8a, one of the interesting features of the SHG of the PBpy is the anisotropy of the SHG concerning the rotation around the Z axis: the point symmetry is C_s with only one mirror in the X–Z plane. This feature strongly suggests that all the PBpy molecules align in a certain direction and the molecule plane tilts from the surface normal. However, the

(18) The number of the clear ED diffraction spots seems to be related to the degree of crystallinity. However, even in the case of PPP, the number of the clear spots depends on delicate experimental conditions for the vacuum deposition (e.g., temperature of substrate).

(19) Brown, C. E.; Kovacic, P.; Wilkie, C. A.; Cody, R. B., Jr.; Kinsinger, J. A. *J. Polym. Sci., Polym. Lett. Ed.* **1985**, *23*, 453 and mass spectra in this reference.

(20) (a) Mo, Z.; Lee, K.-B.; Moon, Y. B.; Kobayashi, M.; Heeger, A. J.; Wudl, F. *Macromolecules* **1985**, *18*, 1972. (b) Bruckner, S.; Porzio, W. *Makromol. Chem.* **1988**, *189*, 961.

(21) (a) Shen, Y. R. *Annu. Rev. Phys. Chem.* **1989**, *40*, 327. (b) Chen, W.; Feller, M. B.; Shen, Y. R. *Phys. Rev. Lett.* **1989**, *63*, 2665. (c) Shen, Y. R. *Nature* **1989**, *337*, 519. (d) Fukuda, T.; Kanbara, T.; Yamamoto, T.; Fujioka, T.; Kajikawa, K.; Takezoe, H.; Fukuda, A. *Mol. Cryst. Liq. Cryst.* **1993**, *226*, 207.

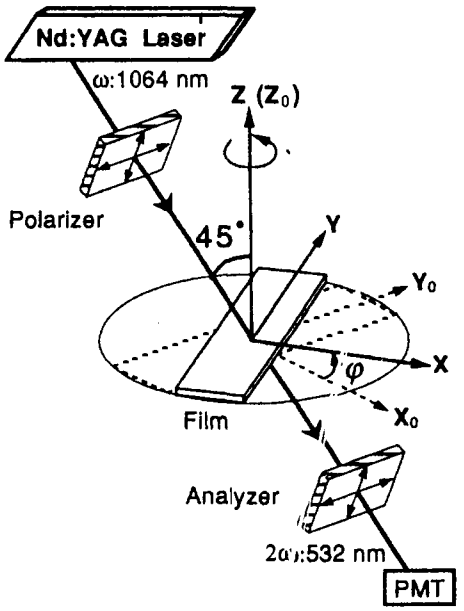

Figure 7. Geometry of the experimen tal system for measuring SHG. Polarized (S and P) light is irradiated to the PBpy film vacuum deposited on the glass substrate which can be rotated around the Z axis. Coordinates (X_0, Y_0, Z_0) are those of the laboratory frame.

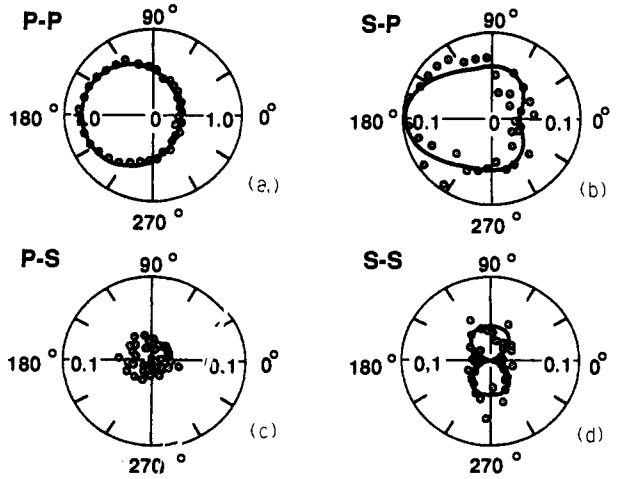

Figure 8. SHG from the PBpy vacuum deposited on the glass substrate for (a) P–P, (b) S–P, (c) P–S, and (d) S–S combinations. Observed data and best theoretical fits are shown by O and —, respectively. The relative scale of the SHG intensity is shown on the radical line. The angle indicates the rotation around the Z axis. The directions giving the minimum SHG and maximum SHG for the P–P combination are taken as 0° and 180°, respectively.

vacuum-deposited PBpy film does not show observable dichroism in its UV–visible spectrum, while alignment of the PBpy molecules in the stretched PVA film is clearly observed (Figure 2, *vide ante*). Therefore, most of the PBpy molecules in the vacuum-deposited PBpy film are not oriented to the certain direction parallel to the surface[22] and the SH light is mainly generated from the interface between the glass substrate and its neighboring layer of PBpy.

Fitting theoretical equations (cf. the supplementary material) to the observed data, with a least-squares method, gives relative values of the six tensor elements for SHG (χ_{XXX}, χ_{XYY}, χ_{XZZ}, χ_{XZX}, χ_{YYZ}, and χ_{ZZZ}); χ_{ZZZ} is the dominant tensor element, and other five elements are 20–50 times smaller than χ_{ZZZ}. The theoretical best-fitted SHG profiles shown in Figure 8 (solid line, at relative values of the tensor elements of $\chi_{XXX} = 6$, $\chi_{XYY} = 3$, $\chi_{XZZ} = 9$, $\chi_{XZX} = 3$, $\chi_{YYZ} = 4$, and $\chi_{ZZZ} = 160$) agree with the observed SHG profiles (O marks), supporting the assumption of the C_s symmetry.

If the PBpy molecules are oriented perpendicularly to the surface of the glass substrate as in the case of the PBpy film vacuum deposited on the carbon substrate, such SHG profiles as those shown in Figure 8 would not be expected. On the contrary, if one assumes an orientation of the PBpy molecules along the surface of the SiO_2 glass as shown in Figure 9a, the molecules are expected to have the component of the dipole moment perpendicular to the surface of the substrate.

The glass substrate is considered to have an acidic Si–O–H groups, and 2,2′-bipyridine, the unit of PBpy, is known to coordinate acidic H to form the s-cis conformation,[23a] in spite of its s-trans conformation in the ordinary state.[23b] A model for the alignment of the PBpy molecules at the interface is depicted in Figure 9, where the PBpy molecules are coordinated to the surface Si–O–H group as depicted in Scheme 3. As described above, the vacuum-deposited PPy film is SHG inactive, which is considered to be due to the difficulty for the PPy molecule to coordinate to the Si–O–H group because of the H–T structure of PPy (*vide ante*). PBpy has a strong ability to coordinate with transition metals whereas PPy does not (*vide infra*).

Treatment of the glass substrate with KOH/methanol followed by treatment with water (cf. the supplementary material) and vacuum evaporation of PBpy to this substrate leads to enhancement of the SHG intensity to about twice without loosing the anisotropy concerning the rotation around the Z axis (Figures 7 and 8a), whereas treatment of the glass substrate with dilute H_2SO_4 causes a decrease in the SHG intensity with loss of the anisotropy. Since the treatment with alkali is considered to increase the concentration of the Si–O–H group and that with acid to have a reverse effect, these results also support the orientation of the PBpy molecules through the coordination to the Si–O–H group. A tilt angle (θ in Figure 9b) can be roughly estimated as 30° from the anisotropic ratio shown in Figure 8a (strongest SHG intensity at 180°/weakest SHG intensity at 0° = ca. 4).[24]

Another interesting feature of the alignment of the PBpy molecules on the glass substrate is that the same anisotropy of the SHG is observed over all of the surface of the glass–PBpy system with an area dimension of 10 × 10 mm, indicating that the PBpy molecules are aligned in the same direction on the surface of the glass substrate as shown in Figure 9. It may be postulated that alignment of several rigidly linear PBpy molecules causes alignment of other molecules coming later.

Fluorescence, Excimer-like Emission, and Other Optical Properties. Powdery PPy and PBpy emit strong green light when irradiated by UV light (365 and 253.7 nm). Figure 10 shows the fluorescence spectra of PPy in a dilute (2.0×10^{-6} mol of monomer unit dm^{-3}) formic acid solution, in a higher concentration (0.5 mol of monomer unit dm^{-3}) of formic acid solution, and as a film on a quartz plate, prepared by spreading a formic acid solution of PPy on the quartz plate and removing the formic acid in vacuo. Steady-state (Figure 10) and time-resolved[25] fluorescence measurements reveal the following characteristics of the fluorescence. (a) The dilute solution (2×10^{-6} M) gives rise to a fluorescence with a maximum at 440 nm (Figure 10a) or 2.82 eV which roughly agrees with the band gap of PPy (2.88 eV, *vide ante*), indicating

(22) The PBpy molecules in the upper layer above the layer neighboring the glass substrate may be aligned perpendicularly to the surface of the substrate. However, ED analysis of the PBpy on the glass substrate has not been possible because of the luck of the thin glass substrate which is transparent to the electron beam and suitable to the ED analysis.

(23) (a) Linnell, R. H.; Kaczmarczyk, A. *J. Phys. Chem.* **1961**, *65*, 1196. (b) Merritt, L. L.; Schroeder, E. D. *Acta Crystallogr.* **1956**, *9*, 801.

(24) Since the P-polarized light is irradiated at 45° to the surface of the PBpy film, the tilt angle θ in Figure 9 is roughly estimated from the ratio between the maximum SHG intensity and the minimum SHG intensity of 4 (Figure 8a) according the equation $\cos(45 + \theta)/\cos(45 - \theta) = 1/4$, which gives the θ value of about 30°.

(25) Ikeda, T.; Lee, B.; Kurihara, S.; Tazuke, S.; Ito, S.; Yamamoto, M. *J. Am. Chem. Soc.* **1988**, *110*, 8299.

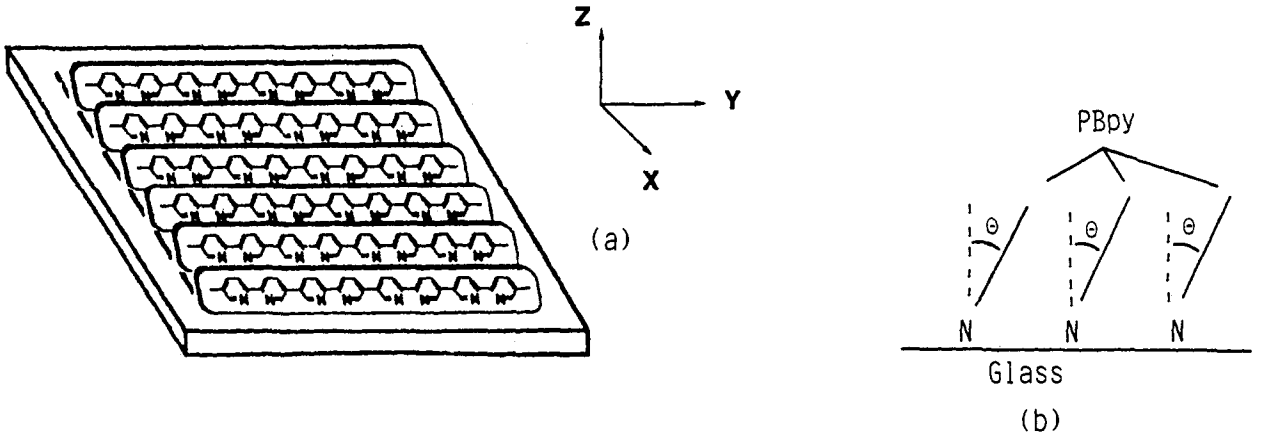

Figure 9. (a) Model for the alignment of PBpy molecules along the direction of the surface. A view of the PBpy molecules from the Y direction is depicted in part b. θ is the tilt angle.

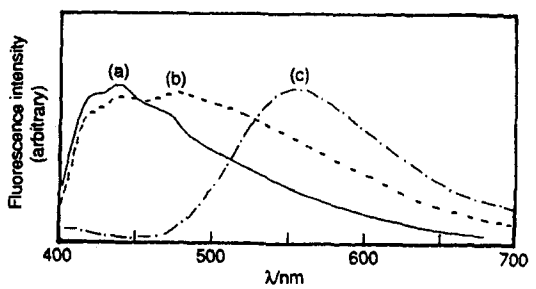

Figure 10. Steady-state fluorescence spectra of PPy (a) in formic acid (2.0×10^{-6} M monomer unit), (b) in formic acid (0.5 M monomer unit), and (c) on a film on a quartz plate, excited at 380 nm.

Scheme 3. Coordination of PBpy Molecules to the Si–O–H Group (Upper Model, a). In the Case of PPy, Such Coordination Does Not Take Place (Lower Model, b)

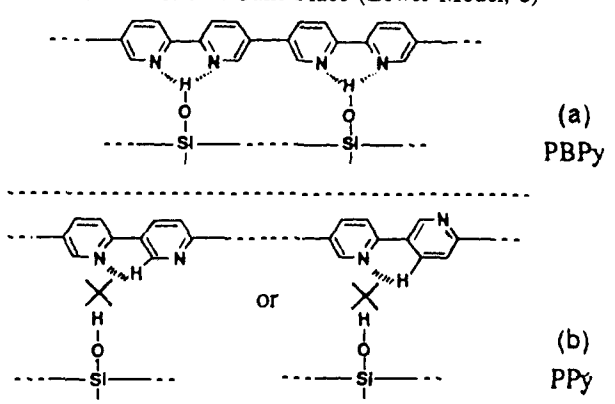

that the fluorescence takes place by migration of electrons from the conduction band to the valence band. The energy difference between the absorption and fluorescence maxima is 2900 cm^{-1}. An excitation spectrum of the dilute solution shows a peak at the position of the π–π^* transition (λ = 373 nm). (b) When the concentration is increased to 0.5 M (Figure 10b), the fluorescence spectrum exhibits a contribution from fluorescence at longer wavelength (presumably centered at about 550 nm). A further increase in the concentration of PPy was not possible owing to limited solubility. When PPy forms a film, it gives rise to the fluorescence with a peak at the longer wavelength, 550 nm (Figure 10c). PBpy film also shows a similar fluorescence with a peak at 535 nm. (c) The fluorescence lifetime measurement indicates that the fluorescence decay of the dilute PPy solution (2×10^{-6} M) is composed mainly of two components with lifetimes of t = 60 and 250 ps when monitored at 440 nm. At the higher concentration (0.5 M), the fluorescence decay is triple-exponential with lifetimes (t) of <10, 90, and 300 ps when monitored at 440 nm. In this case, the time-resolved fluorescence monitored at 570 nm gives a rise component with a lifetime of $t < 10$ ps as well as decay components with lifetimes of t = 90 and 350 ps.

These results, especially the agreement in the lifetimes between the fast decay component at 440 nm and the rise component at 570 nm and between the slow components at both wavelengths, strongly suggest the formation of excimer; a model for its formation is depicted in Figure 11b. On absorption of UV light in the solution with the higher concentration, the linear PPy molecule seems to form the excimer-like adduct with another linear molecule in 10 ps as shown in Figure 11b, and the excimer-like adduct seems to emit the light with the longer wavelength.

The concentration of 0.5 M monomer unit (Figure 11b) corresponds to about 0.01 M PPy and an average distance of 5.5 nm between the centers of two neighboring PPy molecules, whereas the lower concentration (2×10^{-6} M monomer unit, Figure 11a) gives the average distance of 350 nm. Since the PPy molecules with the degree of polymerization of about 50 correspond to the length of about 20 nm, the PPy molecules seem to interact sterically to some extent even before the irradiation of the light in the higher concentration solution.

The fluorescence spectra of P3MePy and P6HexPy exhibit peaks at somewhat shorter wavelengths than that of PPy, 420 and 415 nm, respectively, in formic acid at a low concentration (2×10^{-5} M monomer unit), and these emissions are also attributed to the emission from the single polymer molecule. The fluorescence spectrum of P3MePy at a higher concentration (0.1 M monomer unit) in formic acid shows overlapping of the emission at 420 nm with another emission band centered at about 500 nm, which is also attributed to the excimer-like emission as in the cases of PPy and PBpy. In the fluorescence spectrum of a P3MePy film on a quartz plate, the emission band centered at 500 nm becomes the major emission band; however, the band is clearly overlapped with a smaller emission band at 420 nm in contrast to the case of the PPy film (Figure 10c), suggesting that the P3MePy film gives not only the excimer-like emission but also the emission from the single P3MePy molecule presumably due to the molecularly less ordered structure of P3MePy than that of PPy, which leads to weaker interaction between the molecules to cause the excimer-like emission.

PBpy and P3MePy films are THG (optical third-harmonic generation) active and give the $\chi^{(3)}$ values of 1.5×10^{-11} and 0.5×10^{-11} esu, respectively, at $3h\nu$ of about 18 000 cm^{-1}.

Doping and Electrically Conducting Properties. Figure 12 exhibits the cyclic voltammogram (CV curve) of PPy film laid on a platinum electrode. PBpy film essentially gives the same CV curve. As shown in Figure 12, reduction or n-doping of PPy

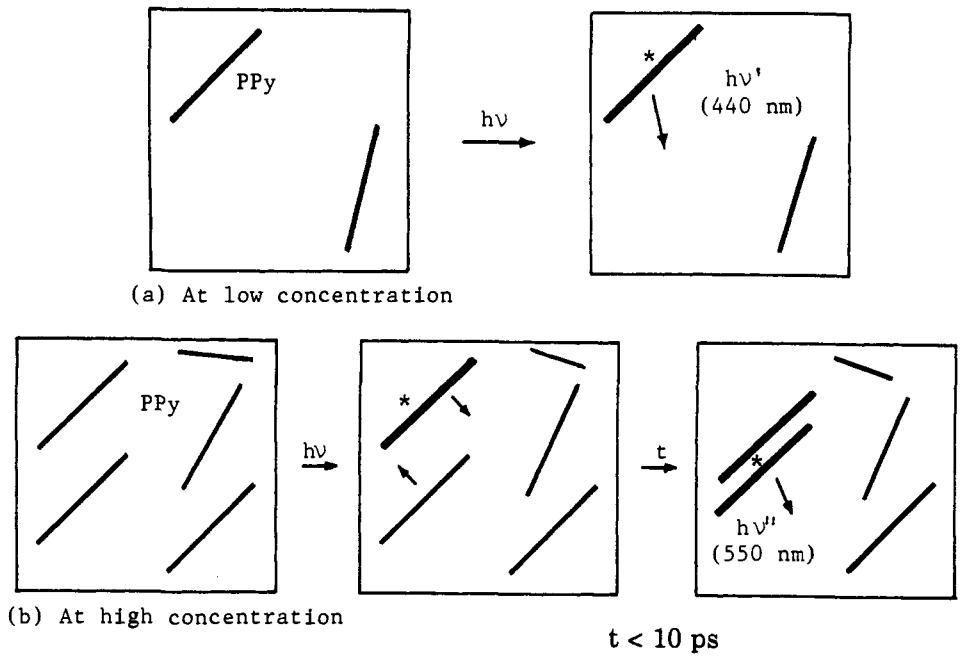

Figure 11. Fluorescence of solutions containing (a) a low concentration (e.g., 2×10^{-6} M monomer unit) and (b) a high concentration (e.g., 0.5 M) of PPy (excimer-like emission).

starts about −1.9 V *vs* Ag/Ag$^+$ (0.34 V *vs* SCE[26]) and E_{pc} appears at −2.43 V.

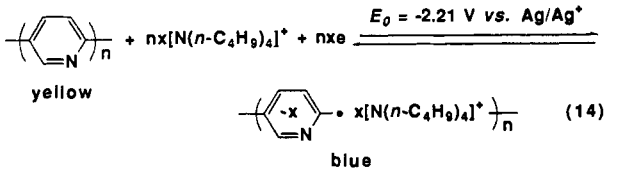

(14)

The averaged value of E_{pc} and E_{pa}, which is taken as the E_0 value, is −2.21 V *vs* Ag/Ag$^+$, and this value is higher by about 0.4 V than the E_0 value of PPP observed in the presence of $[N(n\text{-}C_4H_9)_4][ClO_4]$,[27] indicating that PPy is more easily reduced or n-doped than PPP. Use of $NaBF_4$ (0.1 M) instead of $[N(n\text{-}C_4H_9)_4]BF_4$ gives a reddish purple n-doped PPy at almost the same E_0 value. The difference in the color between the $[N(n\text{-}C_4H_9)_4]^+$- and Na^+-doped (see also the color of chemically Na-doped PPy, eq 15 (*vide infra*)) PPy may be attributed to a delicate difference in an interaction mode of the cations with n-doped PPy.

The UV–visible spectrum of the n-doped PPy film (thickness = ca. 50 nm) on an ITO (indium tin oxide) glass electrode shows appearance of a new absorption band at 515 nm and a very broad absorption toward the near-infrared at −2.0 V *vs* Ag/Ag$^+$ (electrolyte: 0.1 M $[NEt_4][ClO_4]$ in CH_3CN). At −2.3 V *vs* Ag/Ag$^+$, the new absorption band is shifted to 465 nm and the very broad absorption toward the near-infrared becomes much stronger. Formation of polaron and/or bipolaron[1] seems to be responsible for the two new absorption bands. The positions of the two new absorption bands show a difference from those of absorption bands (λ_{max} = 555 and 830 nm)[28] of the cation radical of bpy (Na^+bpy^-).

In contrast to the easy n-doping, PPy is electrochemically inactive in the anodic sweep range (0–1.7 V *vs* Ag/Ag$^+$), whereas PPP and PTh show oxidation or p-doping peaks at 1.10–1.34[26c,27] and 0.71 V, respectively. For comparison, reported oxidation and reduction (or p- and n-doping) potentials of PPP and PTh are shown in Figure 12.

These electrochemical behaviors of PPy and PBpy are consistent with the π-electron-deficient properties of the pyridine ring and the chemically lower reactivity of pyridine toward electrophiles such as NO_2^+ than benzene,[29a] in spite of certain electron-donating properties of pyridine due to the lone pair electrons on nitrogen. UPS (UV photoelectron spectroscopy) analysis as well as band calculations also reveal the electron-accepting properties of PPy.[29b] Electrochemical behaviors of molecules having large π-conjugation systems and those of polymer-modified electrodes are the subject of recent interest.[1a-i,30]

Table 2 summarizes the CV data of PPy and related polymers. By introducing the CH_3 and hexyl substituents, the electrochemical reduction becomes somewhat more difficult by about 0.15–0.3 V presumably due to the shortening of the effective π-conjugation length and/or electron-donating effect of the alkyl substituent.

As shown in eq 14, the n-doping of PPy is accompanied by a color change (electrochromism). PPy (and also PBpy), PMePy's, and P6HexPy are yellow, brownish yellow, and brownish yellow, respectively, whereas the n-doped PPy (and also PBpy), PMePy's, and P6HexPy show the colors of blue, dark blue, and dark orange, respectively.

The doping level (x in eq 14) of PPy and related polymers listed in Table 2 is about 0.3. The peak n-doping current as well as the peak n-undoping current is proportional to the scanning rate, indicating that all of the molecules in the PPy and related polymer films participate in the electrochemical reaction and the electric current is controlled by the mass of the polymer. The n-doping and n-undoping can be cycled for more than 50 times without an observable change of the CV curve for P6HexPy, whereas scanning of the PPy and PBpy films several times leads

(26) (a) Tomot, R.; Zecchin, S.; Schiavon, G.; Zotti, G. *J. Electroanal. Chem. Interfacial Electrochem.* **1988**, *252*, 215. (b) Schiavon, G.; Zotti, G.; Bontempelli, G. *J. Electroanal. Chem. Interfacial Electrochem.* **1985**, *194*, 327. (c) Schiavon, G.; Zotti, G.; Bontempelli, G. *J. Electroanal. Chem. Interfacial Electrochem.* **1984**, *161*, 323.

(27) Yamamoto, T.; Wakayama, H.; Fukuda, T.; Kanbara, T. *J. Phys. Chem.* **1992**, *96*, 8677.

(28) (a) Kaizu, Y.; Kobayashi, H. *Bull. Chem. Soc. Jpn.* **1972**, *45*, 470. (b) Bernier, P. In *Handbook of Conductive Polymers*; Skotheim, T. A., Ed.; Marcel Dekker: New York, 1986; Vol. II, p 1099.

(29) (a) Newkome, G. R.; Paudler, W. W. *Contemporary Heterocyclic Chemistry*; John Wiley: New York, 1982. (b) Seki, K.; Tanaka, H.; Ohta, T.; Sanechika, K.; Yamamoto, T. *Chem. Phys. Lett.* **1991**, *178*, 311.

(30) (a) Jehoulet, C.; Obeng, Y. S.; Kim, Y.-T.; Zhou, F.; Bard, A. J. *J. Am. Chem. Soc.* **1992**, *114*, 4237. (b) Anson, F. C.; Blauch, D. N.; Saveant, J.-M.; Shu, C. F. *J. Am. Chem. Soc.* **1991**, *113*, 1922. (c) Shu, C.-F.; Anson, F. C. *J. Am. Chem. Soc.* **1990**, *112*, 9227. (d) Fischer, J. E.; Heiney, P. A.; Smith, A. B., III. *Acc. Chem. Res.* **1992**, *25*, 112.

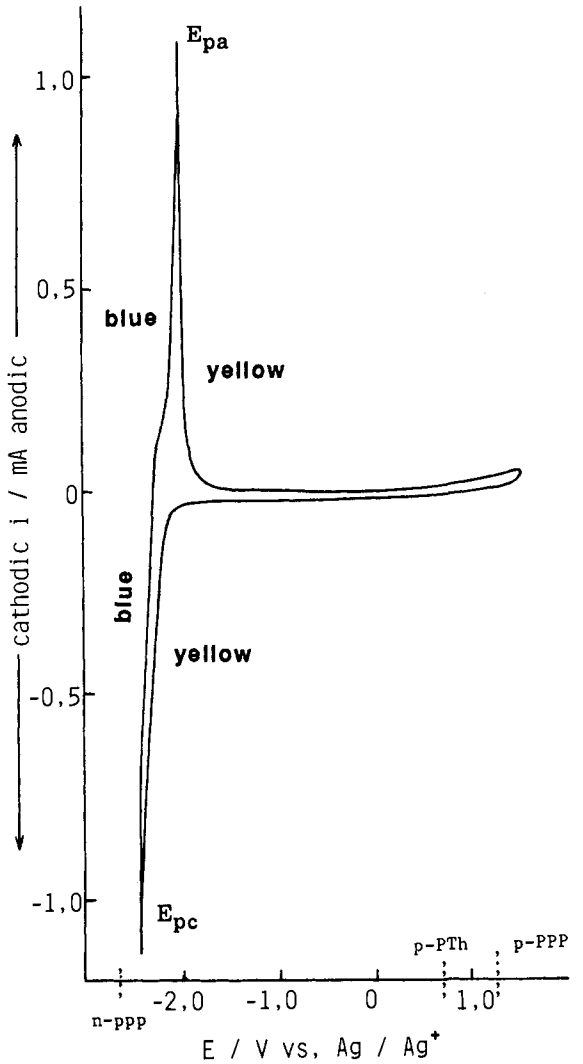

Figure 12. Cyclic voltammogram of PPy film laid on a Pt electrode: acetonitrile solution containing 0.1 M $[N(n\text{-}C_4H_9)_4][BF_4]$; room temperature under N_2; scan rate of 60 mV s^{-1}. Potentials for n-doping of PPP, p-doping of PTh, and p-doping of PPP are also shown.

Table 2. n-Doping Behavior of PPy and Related Polymers[a]

	PPy	PBpy	P3MePy	P4MePy	P6MePy	P6HexPy
E_0,V *vs* Ag/Ag^+	−2.21	−2.21	−2.34	−2.39	−2.37	−2.48

[a] Measured with the polymer film laid on a platinum electrode at room temperature. Solvent was acetonitrile. Electrolyte was $[N(n\text{-}C_4H_9)_4][BF_4]$ for PPy, PBpy, and P6HexPy and $[NEt_4][ClO_4]$ for PMePy's.

to appearance of unidentified small pair peaks at about −1.9 V (cathodic) and 1.3 V (anodic) *vs* Ag/Ag^+, which suggests some structural and/or chemical change of the PPy film. However, the unidentified peaks disappeared after about 25th scanning.

The π-electron-deficient nature of PPy and related polymers revealed by the electrochemical analysis is consistent with the following results of chemical doping of the polymers.

The polymers themselves are insulators with electrical conductivity (σ) of below 10^{-14} S cm^{-1}. However, sodium doping of PPy with sodium naphthalide affords a reddish purple n-doped powder, which has the σ value of 1.1×10^{-1} S cm^{-1} as measured with a compressed powder.

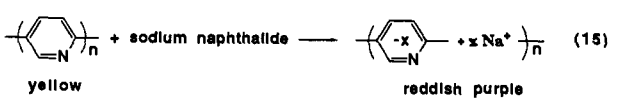

The n-doping with sodium leads to broadening of the IR peaks of PPy, such broadening being usually observed for doped polymers.[1] PBpy and PMePy's exhibit similar color changes by treatment with sodium naphthalide, and the obtained n-doped powders have the σ values of 1.6×10^{-1} and ca. 1×10^{-4} S cm^{-1}, respectively. The n-doped state of the polymers is stable under nitrogen and vacuum. However, exposure of the reddish purple Na-doped PPy to air causes rapid color change to the original yellow of PPy, revealing that the n-doped state is sensitive to oxygen and/or moisture in air. Na-doped P6HexPy is also air-sensitive; however, in this case, the color change is somewhat slower compared with the Na-doped PPy and takes several minutes.

The ESR spectrum of the Na-doped PPy shows two overlapped symmetrical signals at $g = 2.0028$ at room temperature: one broad signal with ΔH_{pp} (peak-to-peak width) of 3.10 mT and relative peak height of 1 and another sharp signal with ΔH_{pp} of 0.34 mT and relative peak height of 1.2. The g-value is comparable to the g-value (2.0026) of the bpy anion radical (K^+bpy^-).[28a] The ΔH_{pp} value of the broad signal is larger than that of the bpy anion radical,[28a] which may be accounted for by coupling with many nitrogens and hydrogens in PPy. On the other hand, the appearance of the relatively sharp signal may be attributed to the presence of rapidly moving or exchanging radical species, which often give rise to a sharp ESR signal due to motional or exchange narrowing.[1a,28b] A detailed discussion of the ESR data of the Na-doped PPy will be given elsewhere.

In contrast to the facile chemical n-doping of PPy by treatment with the reductant, treatment of PPy with AsF_5, which serves as a strong oxidant and oxidizes PPP to give p-doped PPP,[1,2c] does not give the electrically conducting properties to PPy. Reactions of PPy with AsF_5, BF_3·OEt_2, and I_2 give the corresponding adducts, e.g.

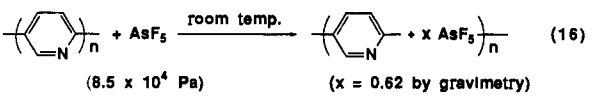

However, the adducts are insulators or have only minor conductivity, showing the σ values of 9.7×10^{-12} and 4.3×10^{-7} S cm^{-1} for the AsF_5 and iodine (0.77 g of iodine/1 g of PPy) adducts, respectively. AsF_5 seems to form the adduct through the lone pair electrons of the nitrogen of PPy and not to abstract π-electrons from the π-conjugation system of PPy because of the π-electron-deficient nature of PPy. On the other hand, as previously reported,[1,2c] PPP can release the π-electrons upon interaction with AsF_5 to give the p-doped state showing the conducting property. The IR spectrum of the iodine adduct of PPy is essentially the same as that of PPy, whereas the formation of the adducts with AsF_5 and BF_3 causes changes in the IR spectrum of PPy. For example, the skeletal vibration bands (1590 and 1430 cm^{-1}) of PPy become more complicated to give rise absorption bands at about 1640, 1600, 1570, and 1440 cm^{-1} presumably due to the formation of the adduct through nitrogen, and they also show new strong and broad absorption bands which seem to originate from AsF_5 (600–800 cm^{-1}) and BF_3 (1000–1150 cm^{-1}),[31] respectively. A similar change of the IR pattern in the skeletal vibration range (1400–1650 cm^{-1}) is observed with an HCl adduct of PBpy.

Transition-Metal Complexes of PBpy and P6HexBpy and Related Chemistry. Since 2,2′-bipyridine, the unit of PBpy, forms a variety of complexes with transition metals, it seems interesting to make transition metal complexes of PBpy and P6HexBpy and reveal basic chemical and physical properties of the complexes of the electrically conducting chelating polymer ligand. The role of PBpy as chelating ligand has been briefly reported in communications.[12c,d]

(31) Pouchert, C. J. *The Aldrich Library of Infrared Spectra*, 2nd ed.; Aldrich Chemical Co. Inc.: Milwaukee, WI, 1975; No. 1328B.

Treatment of PBpy with $FeSO_4$ and $RuCl_3$ (in a 3:1 ratio) in aqueous and ethanolic solutions, respectively, afforded reddish brown and dark brown precipitates, respectively, presumably due to gelation through formation of intermolecular chelate complexes. The color of the precipitate obtained in the treatment with Fe^{2+} resembled the wine red color of $[Fe(bpy)_3]^{2+}$. However, the color of the precipitate obtained in the treatment with $RuCl_3$ was different from that of $[Ru(bpy)_3]^{2+}$, suggesting that the electronic state of Ru or the ligand in the polymer complex was different from those in $[Ru(bpy)_3]^{2+}$. Treatment of PPy with $FeSO_4$ did not cause an apparent color change, in accord with the postulated H–T structure of PPy (*vide ante*).

The reaction of powdery PBpy with $[Ru(bpy)_2Cl_2]$ (1 mol per mol of the bpy unit of PBpy) in water under reflux and removal of water-soluble materials by repeated washing with water gave the following light orange PBpy–Ru complex.

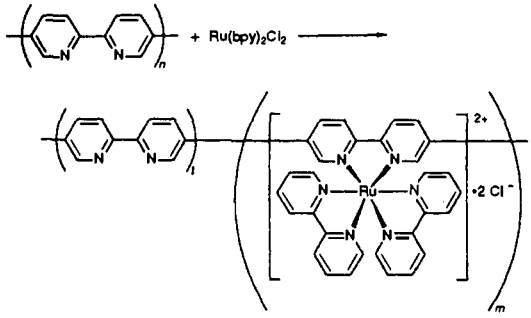

(17)

A part of the PBpy–Ru complex in the crude reaction product is extractable by methanol, and the UV–visible spectrum of the methanol solution gives rise to an absorption band at about 450 nm overlapped with a tail of the π–π^* absorption of PBpy at 373 nm. $[Ru(bpy)_3]Cl_2$ reportedly shows an MLCT absorption band at 452 nm,[32a,b] and the observation of the absorption band at about 450 nm supports the complex formation expressed by eq 17. The Ru content in the methanol-soluble part is about 20 mol % as estimated from the relative intensities of the π–π^* and MLCT bands. The absorption band of $[Ru(bpy)_2Cl_2]$ (515 nm in methanol) was not observable in the UV–visible spectrum of the methanol-extractable fraction. The photoluminescence spectrum of the methanol-extractable fraction gives rise to a strong emission band at 640 nm, which is compared with an emission band of $[Ru(bpy)_3]Cl_2$ (610 nm). No other emission band was observable in the visible region.

Microanalysis of Ru and Cl for samples after removal of the methanol-soluble part indicates 1.3 and 1.4 mol % of Ru per bpy unit of PBpy after 10 and 40 h, respectively, and the molar ratio between Ru and Cl is 1:2. It is reported that labile $[Ru(bpy)_2Cl_2]$[33,34] forms complexes with polymer ligands like poly(4-vinylpyridine)[33,34a] under similar conditions.

PBpy is converted into a semiconducting material ($\sigma = 10^{-5}$ S cm^{-1}) by formation of a complex with Ru, implying generation of carrier(s) in the polymer chain.

When the complex formation was carried out with a thin PBpy film (thickness = 100 nm) laid on a Pt or ITO (indium tin oxide) glass plate, the light orange film obtained contains about 10–15 mol % of Ru per bpy unit as estimated by X-ray photoelectron spectroscopy (XPS). Similar $[Ru(bpy)_2Cl_2]$-treated PBpy film

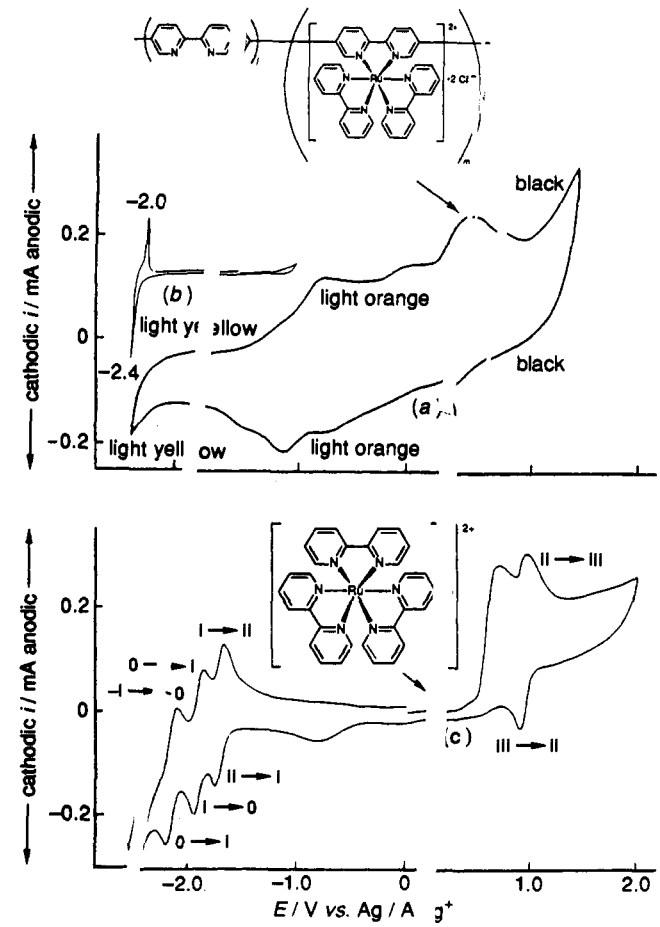

Figure 13. CV curves of (a) the PBpy–Ru(bpy)$_2$ film on a Pt electrode, (b) PBpy film, and (c) $[Ru(bpy)_3]^{2+}$ under N$_2$ in an acetonitrile solution containing 0.1 M $[N(n\text{-}C_4H_9)_4][ClO_4]$. Scan rates were (a) 100 mV s^{-1} and (b) 60 mV s^{-1}.

on a quartz plate gives rise to, in the ti[illegible] absorption of PBpy, a shoulder absorption at about 450 nm as[illegible] signable to the PBpy–Ru complex ; however, the absorption due[illegible] to $[Ru(bpy)_2Cl_2]$ is not observable in the UV–visible spectrum[illegible] of the film.

The PBpy film laid on Pt and contai[illegible]ining the complex shows peaks due to redox reactions of the PBpy–Ru complex in cyclic voltammetry (CV) [curve (a) in Figure 13]. The CV cycle was repeated without any observable change for more than 10 times. The redox peaks of PBpy at about –2.2 V *vs* Ag/Ag^+ are weakened or are not observable in the CV chart of the PBpy–Ru film, indicating a profound change in the electronic state of PBpy, whereas the CV chart of the PBpy–Ru film shows several new peaks, which are considered to arise from the presence of coordinated $Ru(bpy)_2$ centers.

Figure 13c shows the CV curve of the corresponding low molecular mass complex, $[Ru(bpy)_3]Cl_2$.[32a] It is seen from Figure 13 that (i) the redox peaks of $[Ru(bpy)_3]^{2+}$ related to ligand-based radical anions are shifted to higher potentials in the PBpy–Ru complexes whereas the $Ru^{II} \rightleftharpoons Ru^{III}$ redox peaks are shifted to lower potentials and (ii) all the redox peaks are broadened. These results suggest the presence of electronic interactions between the Ru species through the electrically conducting polymer chain. These CV results are in sharp contrast to those obtained with a $Ru(bpy)_2L_2$ type complex attached to a non-conjugated polymer ligand (e.g., poly(4-vinylpyridine)),[34d] the CV curves of the attached complex groups showing the redox peaks at almost the same position as in the corresponding monomer complex.

Thus, the PBpy–Ru complex presents a unique redox behavior which is considered to be characteristic of the metal complexes of electrically conducting π-conjugated polymer ligands. Similar

(32) (a) Tokel-Takvoryan, N. E.; Hemingway, R. E.; Bard, A. J. *J. Am. Chem. Soc.* **1973**, *95*, 6582. This paper shows a CV of $[Ru(bpy)_3](ClO_4)_2$ and describes the dichloride salt, which shows irreversible oxidation at about 1.16 V (*vs* SCE) in accord with Figure 13b. (b) Mabrouk, P. A.; Wrighton, M. S. *Inorg. Chem.* **1986**, *25*, 526.

(33) Ramaraj, R.; Natarajan, P. *J. Polym. Sci., Polym. Chem. Ed.* **1991**, *29*, 1339.

(34) (a) Hayes, M. A.; Meckel, C.; Schatz, E.; Ward, M. D. *J. Chem. Soc., Dalton Trans.* **1992**, 703. (b) Calvert, J. M.; Meyer, T. J. *Inorg. Chem.* **1982**, *21*, 3989. (c) Durham, B.; Walsh, J. L.; Carter, C. L.; Meyer, T. J. *Inorg. Chem.* **1980**, *19*, 860. (d) Samuels, G. J.; Meyer, T. J. *J. Am. Chem. Soc.* **1981**, *103*, 307.

Table 3. Photoevolution of H_2 from Aqueous Media[a]

run	catalyst[b]	amount of H_2 evolved (μmol) with NEt_3[c]	without NEt_3[d]
1	PPy–$RuCl_3$	39	
2	PBpy	1	0
3	PBpy–$RuCl_3$	137	0
4	complex obtained from the [PBpy–Ru(bpy)$_2$Cl$_2$] system (eq 17) (MeOH-insoluble part)	4	trace
5	PBpy–RuO_2		0.2 trace[e]
6	[PBpy–Ru(bpy)$_2$Cl$_2$] system–RuO_2		1.5 0.06[e]
7	RuO_2		trace

[a] A reaction time of 6 h and a 500-W Xe lamp (>300 nm) were used. In all cases, light was irradiated from the same distance. [b] The amount of the polymer or the complex was 20 mg. The amount was 3.6 mg for runs 1 and 3: 0.05 mol/mol of monomer unit of PPy (run 1) and 0.1 mol/mol of monomer unit of PBpy (run 3), respectively. In the case of run 4, the complex prepared after 10 h of reflux (see text) was used. The amount of RuO_2 for runs 5 and 6 was 1.8 mg. [c] In a mixture of H_2O (1 mL), methanol (1 mL), and triethylamine (1 mL). [d] In a mixture of H_2O (1.5 mL) and methanol (1.5 mL) unless otherwise noted. [e] In water.

behavior was reported for an $Fe^{II} \rightleftharpoons Fe^{III}$ redox reaction in poly(ferrocene-1,1′-diyl),[35a] which is electrically conductive and undergoes rapid electron exchange in a mixed valence state.[35b]

Recently Yanagida and his co-workers reported the high catalytic activity of a mixture of PPy and $RuCl_3$ for photoevolution of hydrogen from water.[36] Since PPy has only a low coordinating ability toward transition metals compared with that of PBpy, the use of the PBpy–$RuCl_3$ system is expected to have a stronger effect due to the complex formation on the photoevolution of hydrogen from water.

Table 3 summarizes the results. The PPy–$RuCl_3$ system (run 1) showed catalytic activity essentially the same as that reported by Yanagida and his co-workers.

On the other hand, the PBpy–$RuCl_3$ system (run 3) shows activity about 3.5 times higher than that of the PPy–$RuCl_3$ system, indicating the important role of the coordination of Ru to PBpy. On the contrary, the PBpy–Ru complex obtained by eq 17 (run 4 in Table 3) showed lower catalytic activity.

The difference in the catalytic activity between the PBpy–$RuCl_3$ system and the PBpy–$[Ru(bpy)_2]^{2+}$ complex may be due to the difference in the density of the Ru species in the surface region of the PBpy polymer particles or to the difference in the catalytic activity between the Ru species formed. Photochemical redox reactions of molecules are subject of recent interest,[37] and photogeneration of H_2 from water by heterogeneous systems containing Ru–bpy complexes has been reported.[37d] In the presence of a RuO_2 catalyst, the catalytic system exhibits higher activities toward the photoreduction of water in the absence of the sacrificing reagent NEt_3 (runs 5 and 6), and evolution of H_2 even in the absence methanol is observed (run 6) though the amount is small.

PBpy also forms a complex with $NiCl_2$. A reaction of powdery PBpy and a DMF solution of $NiCl_2$ under N_2 affords a yellow complex whose elemental analysis indicates 39 mol % of the bpy unit of PBpy forms the complex with $NiCl_2$. Taking a larger

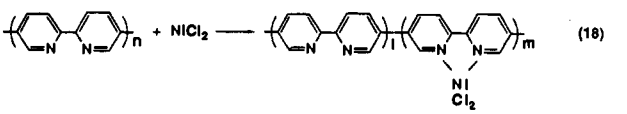

(18)

amount of $NiCl_2$ than $Ru(bpy)_2^{2+}$ agrees with the reported high coordinating ability of Ni^{2+} to bpy. By the formation of a complex with $NiCl_2$, the skeletal vibrations (1587 and 1453 cm^{-1}) as well as the in-plane δ_{C-H} vibrations (1072 and 1025 cm^{-1}) of PBpy are shifted to higher frequency by about 10–15 cm^{-1}. Since similar shifts are observed for the formation of a complex of bpy with $NiCl_2$, the shift of the IR bands supports the formation of the PBpy–$NiCl_2$ complex. The complex has an electrical conductivity of 1×10^{-7} S cm^{-1}.

The CV curve of the PBpy–$NiCl_2$ complex[38] in a CH_3CN solution of $[N(n\text{-}C_4H_9)_4][BF_4]$ exhibits, besides the n-doping and n-undoping peaks of PBpy, redox peaks in a range of −1.0 V to −2.0 V *vs* Ag/Ag^+, where the redox reactions of $NiBr_2$(bpy) also take place as observed in the CV curve of $NiBr_2$(bpy). The redox peaks of the PBpy–$NiCl_2$ complex are broadened compared with those of $NiBr_2$(bpy), suggesting occurrence of electron exchange between Ni species through the backbone π-conjugation system of PBpy, similar to the case of PBpy–$Ru(bpy)_2$. One of the interesting electrochemical properties of the PBpy–Ni complex is that reduction of the PBpy–Ni complex in a CO_2 atmosphere (1 atm) causes an irreversible flow of reducing electric current at room temperature with a peak cathode potential of −2.15 V *vs* Ag/Ag^+. This is characteristic of the electrochemical reduction of Ni complexes in the CO_2 atmosphere and related to the electrochemical reduction of CO_2 by the PBpy–Ni complex. Actually, evolution of CO (ca. 0,3 mol/1 mol of electron) is observed after the electrochemical reduction under CO_2 at a constant potential of −2.40 V *vs* Ag/Ag^+. The film of the PBpy–Ni complex was stable during the electrochemical reduction of CO_2. Recently many papers have been published on electrochemical reduction of CO_2 with Ni complexes.[39]

The complex formation reaction of P6HexBpy with transition metals proceeds in solutions and can be followed by UV–vis spectroscopy. A mixture of P6HexBpy and $Ni(cod)_2$ gives rise to an absorption band at 635 nm, which is shifted from the MLCT bands of Ni(cod)(bpy) at 570, 800, and 890 nm. The UV–vis spectrum of a P6HexBpy–$Fe(bpy)_2Cl_2$ system in $CHCl_3$ is considerably different from that of the bpy–$Fe(bpy)_2Cl_2$ system in $CHCl_3$. In the case of the bpy–$Fe(bpy)_2Cl_2$ system, addition of bpy to a $CHCl_3$ solution of $Fe(bpy)_2Cl_2$ leads to an increase in the absorbance of a peak at 520 nm (peak position of $[Fe(bpy)_3]^{2+}$)[40] with an isosbestic point at 575 nm. In the case of the P6HexBpy–$Fe(bpy)_2Cl_2$ system, on the contrary, addition of P6HexBpy to the $CHCl_3$ solution does not lead to the appearance of a new absorption band around 520 nm but it causes an increase in the absorbance in a range from 550 nm toward the near-infrared. The UV–vis observation of the P6HexBpy–$Fe(bpy)_2Cl_2$ system suggests formation of unique electronic state(s) by coordination of $Fe(bpy)_2^{2+}$ to P6HexBpy, and the increase in the absorption in the range from 550 nm toward the near-infrared may be attributed to formation of polaron or bipolaron in the P6HexBpy polymer chain.

Conclusion

Dehalogenation polycondensation of the corresponding dihalogenated monomers based on organonickel chemistry[6] gives soluble PPy, PBpy, and their alkyl derivatives. PPy and PBpy take a rigidly linear structure in formic acid, and the orientation of PPy and PBpy molecules in stretched PVA film as well as in

(35) (a) Oyama, N.; Takizawa, Y.; Matsuda, H.; Yamamoto, T.; Sanechika, K. *Denki Kagaku* **1988**, *56*, 781. (b) Yamamoto, T.; Sanechika, K.; Yamamoto, A.; Katada, M.; Motoyama, I.; Sano, H. *Inorg. Chim. Acta* **1983**, *73f*, 175.

(36) (a) Matsuoka, S.; Kohzuki, T.; Nakamura, A.; Pac, C.; Yanagida, S. *J. Chem. Soc., Chem. Commun.* **1991**, 580. (b) Maruo, K.; Yasuda, N.; Wada, Y.; Yanagida, S. *Chem. Lett.* **1992**, 1951. (c) Matsuoka, S.; Kohzuki, T.; Kuwana, T.; Nakamura, A.; Yanagida, S. *J. Chem. Soc., Perkin Trans. 2* **1992**, 679.

(37) (a) Serpone, N.; Pelizzetti, E., Eds. *Photocatalysis-Fundamentals and Applications*; Wiley Interscience: New York, 1989. (b) Fox, M. A.; Dulay, M. T. *Chem. Rev.* **1993**, *93*, 341. (c) Bard, A. J. *Ber. Bunsen-Ges. Phys. Chem.* **1988**, *92*, 1187. (d) Cooke, M. C.; Homer, J.; Jarvie, A. W. P.; Miller, J. D. *J. Chem. Soc., Chem. Commun.* **1984**, 1202.

(38) Prepared by a reaction of PBpy film laid on Pt electrode with a DMF solution of $NiCl_2$ (*cf.* the supplementary material).

(39) E.g.: Derien, S.; Dunach, E.; Perichon, J. *J. Am. Chem. Soc.* **1991**, *113*, 8447.

(40) Ehrenfreuend, M.; Leibenguth, J.-L. *Bull. Soc. Chim. Fr.* **1970**, 2494.

film vacuum deposited on carbon and glass substrates reveals basic properties of such linear rodlike molecules. The excimer-like emission from PPy and PBpy is also related to their linear structure.

PPy, PBpy, and their derivatives are chemically and electrochemically n-doped due to the π-deficient nature of the pyridine ring containing the electron-withdrawing imine nitrogen. PBpy and P6HexBpy form complexes with transition metals, and the Ru complex serves as a catalyst for the photoevolution of H_2 from aqueous solutions. CV analysis of the complex suggests electron exchange between the metal species through the π-conjugation system of the electrically conducting polymer chelating ligand.

Experimental Section

Materials. Solvents were dried, distilled, and stored under N_2. 2,5-Dibromopyridine, 2,5-dichloropyridine, 2,2′-bipyridine, triphenylphosphine, 1,5-cyclooctadiene, and maleic anhydride were purchased from Tokyo Chemical Industry Co. Ltd. $Ni(cod)_2$,[41] $Ni(PPh_3)_4$,[42] $RuCl_2(bpy)_2$,[43] $[Ru(bpy)_3]Cl_2$,[44] $FeCl_2(bpy)_2$,[45] and $NiBr_2(bpy)$[46] were prepared according to literature.

Polymerization. $Ni(cod)_2$ (1.53 g, 5.74 mmol), 1,5-cyclooctadiene (0.62 g, 5.7 mmol), and bpy (0.87 g, 5.8 mmol) were dissolved in 20 mL of DMF in a Schlenk tube under nitrogen. To the solution was added 2,5-dibromopyridine (1.1 g, 4.6 mmol) dissolved in 20 mL of DMF. The reaction mixture was stirred at 60 °C for 2 h to yield a yellow precipitate (run 1 in Table 1). The precipitate was collected by filtration, washed with hot toluene, a warm aqueous solution of ethylenediaminetetraacetic acid (EDTA, pH = 3), a warm aqueous solution of EDTA (pH = 9), a warm aqueous solution of NaOH (pH = 9), warm distilled water, and hot benzene in this order, and dried under vacuum to obtain a yellow powder of PPy. Anal. Found: C, 77.3; H, 3.7; N, 17.7. Calcd. $(C_5H_3N)_n$: C, 77.9; H, 3.9; N, 18.2. IR: 1584 (s), 1452 (vs), 1095, 1024, 1010, 995, 824 (vs), 793, 740 cm^{-1}. $^{13}C\{^1H\}$-NMR (HCOOH, 25 MHz) (chemical shift from DSS (sodium 2,2-dimethyl-2-silapentane-5-sulfonate)): 126–153-ppm complex pattern with peaks at 127, 132, 137, 146, and 148 ppm.

PBpy was prepared analogously. Anal. Found: C, 76.9; H, 4.2; N, 17.9. Calcd $(C_{10}H_6N_2)_n$: C, 77.9; H, 3.9; N, 18.2. IR (KBr): 3050, 3012, 1587 (s), 1453 (vs), 1072, 1025, 995, 831 (vs), 795, 741 cm^{-1}. ^1H-NMR (CF_3COOD, 100 MHz): 10.16 (2H, 6,6′-H), 9.60 ppm (4H, 3,3′- and 4,4′-H). $^{13}C\{^1H\}$-NMR (HCOOH, 25 MHz) (chemical shift from DSS): 147.0, 145.3, 142.6, 135.1, and 124.9 ppm and additional small peaks presumably due to presence of s-cis and s-trans conformations.

Acknowledgment. We are grateful to Drs. T. Kaino, T. Kurihara, and N. Ooba of NTT Optoelectronics Laboratories, Nippon Telegraph and Telephone Corp., for measurement of THG. Thanks are due to Mr. Y. Tsutsumi and Mr. M. Hasegawa of Tosoh Co. Ltd. for measurement of n_D. We also thank Prof. K. Domen, Dr. T. Kanbara, Mr. T. Fujioka, Mr. K. Kajikawa, Mr. N. Saito, and Miss C. Mori for their helpful discussion and experimental support.

Supplementary Material Available: Text describing experimental details of the synthesis of monomers including their analytical and spectroscopic data, synthesis of polymers (other than PPy and PBpy) including their analytical and spectroscopic data, measurements, chemical doping, preparation of metal complexes, and SHG analysis (12 pages). This material is contained in many libraries on microfiche, immediately follows this article in the microfilm version of the journal, and can be ordered from the ACS; see any current masthead page for ordering information.

(41) Wilke, G. *Angew. Chem.* **1960**, *72*, 581.
(42) Schunn, R. A. *Inorg. Synth.* **1972**, *13*, 124.
(43) Sullivan, B. P.; Salmon, D. J.; Meyer, T. J. *Inorg. Chem.* **1978**, *17*, 3334.
(44) Broomhead, J. A.; Young, C. G. *Inorg. Synth.* **1982**, *21*, 127.
(45) Basolo, F.; Dwyer, F. P. *J. Am. Chem. Soc.* **1954**, *76*, 1454.
(46) Sıove, A.; Ades, D.; Chevrot, C. *Makromol. Chem.* **1989**, *190*, 1361.